MET.O.14

METEOROLOGICAL OFFICE
BOUNDARY LAYER RESEARCH BRANCH
TURBULENCE & DIFFUSION NOTE

T.D.N. No. 150

Dispersion Experiments on the windward slope of the hill Blashaval, North Uist.

by

R.H.Maryon, J.B.G.Whitlock and G.J.Jenkins.

October 1984.

Dispersion Experiments on the windward slope of the hill Blashaval, North Uist

1. Introduction

This paper describes short-range dispersion experiments held on the upwind slopes of an isolated, roughly conical hill on the Hebridean island of North Uist in conditions of (largely) neutral stability. The trials were adjunct to the main Blashaval field experiment investigating the influence of an isolated hill upon the mean wind and turbulence, which were conducted by staff of the Met. Office Boundary Layer Research Branch in September 1982 (Mason and King, 1985, henceforth referred to as MK85). Sections 2-4 of the present paper describe the experimental set-up, sections 5-9 deal with the analysis of the horizontal dispersion and sections 10-12 with dispersion in the vertical.

2. The Dispersion Equipment

A direct estimate of the horizontal and vertical dispersion was made using an array of passive diffusion samplers as shown in Figure 1. Two masts of three 5m fibre glass sections were erected just over 50m apart. A horizontal line was passed through an eye attached to the top of each mast. From this line five similar vertical lines were hung. Passive samplers were attached at the heights shown in the figure.

The passive 'badge' samplers were designed and tested at the Chemical Defence Establishment (C.D.E) Porton Down (Bailey and Hollingdale-Smith 1977). The array of samplers was sited approximately 100m up the hillside from the source mast. The release was made at a height of 8m to minimise the influence of irregularities in the local terrain.

The tracer released was Tetrachloroethylene (C_2Cl_4) (a dry cleaning fluid: ICI tradename Perklone) which is a liquid. It was released using a combination of two pieces of commercial spraying equipment:

1) Killaspray - a reservoir of liquid is pressurised to about 30 p.s.i by a small pump. The liquid is forced up a tube to an atomising nozzle.

2) Mist Blower - a stream of air is produced by a fan driven by a two-stroke petrol engine. The tracer is gravity fed into the air flow from a reservoir.

The tubing of both pieces of equipment was lengthened so that the atomising nozzle of the killaspray could be introduced in the air stream of the mist blower at a height of 8m. A fine stream of droplets was produced and fallout was kept to a minimum by the height of the release.

Smoke grenades were used at ground level to ascertain the local wind direction and the need to move either the release position or the sampling array. The 2m wind speed and direction were recorded at the release site.

3. The Dispersion Experiments

Ten experiments were conducted, the tracer being released for periods of 10 to 20 minutes. All but the last were sited on the hillside between the S.E. and the S.W. Figure 2 shows the approximate positions of the experiments. The weather was unusually windy, and often very wet, with extensive cloud cover. Most of the experiments were conducted in a neutral atmosphere but one or two took place in slightly unstable conditions. Only the successful or partially successful hillside runs, experiments 2 to 9, will be dealt with in this paper. Figure 3, extracted from the 1:50000 Ordnance Survey map, shows the country surrounding Blashaval. To the south of the hill the formerly glaciated surface is one of low, heather-clad, often boggy moorland interspersed with extensive areas of peaty lake and sea-loch.

Rough estimates of likely peak dosage were computed for the experiments of greatest interest (Exp. 2, 3, 8 and 9, see Section 6). The classical Gaussian dispersion model was used for this purpose, which for level terrain gives

$$\chi_{peak} = \frac{Q}{2\pi \bar{u} \sigma_y \sigma_z}\left[1 + \exp\left(-\frac{2 z_s^2}{\sigma_z^2}\right)\right]$$

where $\bar{u}$ is the mean windspeed in the x direction, z_s the source height, σ_y, σ_z the standard deviations of the cross-wind and vertical dispersion, which are estimated using nomograms based upon Pasquill stabilities (Smith, 1973). $\bar{\chi}_{peak}$ is the peak concentration, Q the source strength given by

$$Q = \frac{V\rho}{\tau}$$

where V is the volume of tracer released, ρ its density and τ the duration of the release.

The mass of tracer captured by the chemical samplers is obtained from

$$M = \bar{\chi}\tau R$$

where R is the 'uptake rate' (volume per unit time) - in effect a measure of the efficiency of absorption. As for any given experiment τ and R are constant, the mass (i.e. dosage) profile may be taken as similar to the concentration profile. R assumes a diffusive process across the space between the sampler membranes and is considered to be independent of wind strength.

Maximum sampler dosages were estimated using the above formulae and are listed in Table 2 for comparison with the observations in Table 1. The dosages recorded for Exp 2 and 3 appear to be low. However, with σ_y for these experiments at twice the nomogram value, and σ_z well up to the nomogram figures the peak dosage for Exp. 2 is seen to be of the right order, and that for Exp 3 low but not beyond the variability to be expected in an experiment of this kind. Some of the strong wind Exp 8 and 9 dosages

are inexplicably large, and may throw doubt on the presumed independence of R from wind strength. For Exp 9, however, only 1 of the observed dosages is completely incompatible bearing in mind the small σ_y, σ_z which were observed (Table 3). In view of the uncertainties, no quantitative assessments of concentration will be attempted in this paper, but attention confined to the general shape of the profiles.

4. Chemical analysis of the badge samplers

In order to avoid contamination, or loss of tracer after use, the samplers were stored in heat-sealed lamofoil bags. These are made of thin aluminium foil coated on the inside with plastic so that once sealed it is impossible to open without tearing the plastic. The samplers were prepared at C.D.E. and sealed into the bags. At the end of each trial each sampler was replaced and heat-sealed.

The analysis was carried out by chemists at C.D.E. The disc of activated charcoal cloth was removed and eluted with 2 ml of acetone. 1 µl of the elution was injected onto the column of a gas chromatograph. In order to lessen the analysis time two gas chromatographs were used, a Pye 104 with a 5ft column and a Perkin Elmer F11 with a 6ft column. Both columns were packed with 6% Dexsil 300 GC on GCQ as support. The column separation was followed by electron capture detection. The carrier gas was nitrogen flowing at 45 ml/min. The dosage was calculated by comparing the recorded peak heights with the peak produced by injecting a standard solution into the gas chromatograph.

5. Crosswind dispersion over uniform terrain

The various theoretical approaches to the dispersion of airborne pollutants over uniform terrain are outlined in Chapter 3 of Pasquill and Smith, 1983, henceforth PS83. Under the assumptions of stationarity and homogeneity Taylor's statistical theory yields the spectral form

$$\sigma_y^2 = \overline{v'^2} T^2 \int_0^\infty F(\omega) \frac{\sin^2(\pi\omega T)}{(\pi\omega T)^2} d\omega \qquad (1)$$

where σ_y, $\overline{v'^2}^{1/2}$ are the standard deviations of the crosswind displacement of a particle after time T and of its crosswind eddy velocity respectively, and $F(\omega)$ is the normalised Lagrangian spectral function. At short times T the integral approximates unity, so that

$$\sigma_y^2 \simeq \overline{v'^2} T^2 \qquad (2)$$

and the plume is being spread laterally by the entire spectrum of turbulence. The initial spread will reflect, primarily, the high frequency motions. If T is large, the filter $\frac{\sin^2(\pi\omega T)}{(\pi\omega T)^2}$ narrows and emphasises the low frequency part of the spectral function, so that the dispersion is largely determined by the low frequency oscillations. In this case equation (1) is expressed as

$$\sigma_y^2 = 2\overline{v'^2} t_L T \qquad (3)$$

where t_L is the Lagrangian integral time scale. Equations (2) and (3) illustrate the transition from linear to parabolic spread as T increases.

A filter is equivalent to a moving average, and an alternative form of (1) is

$$\sigma_y^2 = \overline{v'^2_{\tau,T}}\,\overline{T}^2 \qquad (4)$$

where $\overline{v'^2_{\tau,T}}$ is the S.D. of the eddy velocity of a particle averaged over a time interval T and, as S.D. is a function of sampling time, sampled over a period τ. This expression is Lagrangian, and its transposition to an Eulerian reference frame, for comparisons with actual turbulence measurements, requires a relation between the Lagrangian and Eulerian autocorrelation functions. This is a difficult and unsolved problem; for present purposes Hay and Pasquill's hypothesis (1959) that

$$R_L(\xi) = R_E(t) \quad \text{where } \xi = \beta t \qquad (5)$$

is adopted. Here, $R_E(t)$ is the Eulerian autocorrelation function which is taken to decay more rapidly than the Lagrangian, $R_L(t)$ with β the ratio of the Lagrangian to the Eulerian time-scales. The hypothesis leads to the relation

$$\sigma_y^2 = \sigma_v^2(\tau, T/\beta)\,\overline{T}^2 \qquad (6)$$

where $\sigma_v(\tau, T/\beta)$ now represents fixed point measurements of the crosswind eddy velocities which are averaged over a time interval T/β during a sampling period τ. Neither differences in the shape of the Lagrangian and Eulerian correlograms, nor a degree of uncertainty in the ratio β are considered critical to the applicability of (6).

Profile measurements such as those made by MK85 suggest that for neutral static stability the condition of homogeneity is effectively satisfied for crosswind eddy motions in the surface stress layer over uniform terrain; dimensional analysis for an elevated release in the surface stress layer yields

$$\frac{\sigma_y^2}{T} = u_*^2 f\left(\frac{z_s}{u_* T}\right) = \sigma_v^2 (\tau, T/\beta)$$

(from (6))

The function f is evidently effectively constant unless T is very small. In the real atmosphere the condition of stationarity, although assumed to apply over short periods, is probably seldom realized. σ_y varies with height, close to a point source, and in processing observed dispersion data expression (6) is taken as applicable to the maximum plume width provided it is fairly close to the level of the centroid of the plume cross-section.

6. Dispersion on a hill slope

Many new factors become involved when a plume disperses over a hill slope. To begin with, the position and height (above the surface) of the source will, with the effective diffusivity, determine whether a plume will be carried onto a hill surface (Hunt et al 1979). For a near-surface release on an upwind slope the matter is not in doubt. The mean flow will be distorted by the hill with the streamlines displaced towards the surface, converging in the vertical and diverging laterally as some of the air is steered around the hill. Off-centre, the air may be forced to converge laterally. These effects are most apparent in stable flows, but are present, if less marked, in neutral conditions. As the distortion of the flow will vary slightly with height above surface, some directional shear may also be imposed. The static stability may be modified. When the

air flow has a low frequency oscillation interaction with the hill may lead to irregular, large-amplitude fluctuations in direction, while in the lee of the hill additional complications, such as separation of the flow, may occur.

Important considerations are the changes in the shear stress profile and turbulent motion as the air is accelerated up the hill. To illustrate this, and to define some terms for use in later sections, figure 4 shows the standard 2-layer configuration of airflow over a hill of slight to moderate slope, as used in the Jackson and Hunt linear asymptotic theory (1975).

The hill is of height h and half-length L. An inner region where turbulent dissipation is in equilibrium with the production by the local shear is of height l ; in an outer region, where the travel time

$$T \simeq \frac{L}{\bar{u}} < t_L$$

the turbulent eddies are distorted by the mean flow over the hill: 'rapid distortion' theory (Britter et al, 1981) is taken to apply here. The thickness of the inner layer can be estimated from

$$1/L \log_e(l/z_o) \simeq 2k^2 \qquad (7)$$

where k is von Karman's constant, z_o the surface roughness estimated at 0.02m. (7) gives a value of about 22m for l over Blashaval, assuming L $\simeq$ 470m for broadly southerly flows. MK85 point out that the transition towards rapid distortion conditions starts as low as $l/2\pi$. Near the surface of the hill summit the ratio of the increase in turbulent motion over the upstream value, $\Delta\sigma_v^2$ to the upstream value, $\sigma_{v,\infty}^2$ can be related to the slope of the hill by the expression

$$\frac{\Delta\sigma_v^2}{\sigma_{v,\infty}^2} = \frac{\delta h}{L}$$

(Britter et al, 1981). This ratio is about 1.7 for Blashaval, but decreases with z and approximates unity as the outer layer is approached. It is no easy matter, then, to determine a 'theoretical' increase in turbulence for a specified value of z even over the hilltop – see MK85 for some measurements and a discussion. As the upstream and summit dimensionless crosswind turbulence spectra ($n S(n)/u_*^2$) at Blashaval are of similar shape and amplitude (MK85), it is reasonable to assume that the 'filtered' (Lagrangian) ratio

$$\frac{\Delta\sigma_v^2(\tau, T/\beta)}{\sigma_{v,\infty}^2(\tau, T/\beta)} \simeq \frac{\Delta\sigma_v^2}{\sigma_{v,\infty}^2} \simeq 1.7 \qquad (8)$$

Over the windward slopes of a hill the ratio might be expected to be intermediate between the upwind and summit values, but its estimation from dispersion measurements is greatly complicated by the other factors described in this section (vide Hunt et al, 1983).

Most of these effects are strongly position-dependent, and the detail of the hill contours taken with the alignment of the mean wind will influence local accelerations and steerage. The difficulties of attempting dispersion experiments over irregular terrain, and the highly qualified character of the results obtained therefrom are immediately apparent. At the present time, little is likely to be learnt using a hillside line of samplers with a point source unless the array axis is set perpendicular to the direction of a reasonably steady wind blowing directly up a forward slope of a symmetric hill – conditions easy to specify, but surprisingly difficult to achieve in practice.

Owing to the difficulty in making last-minute adjustments to the 2-dimensional array of samplers few of the dispersion experiments came near to satisfying these conditions and the experiments were often reduced to making the best of adverse conditions. To add to the severe problem of properly aligning the sampler array were the presence (possibly) of low frequency effects, and a deflection of the mean flow, which the experimenters were in no position to gauge. These effects frequently resulted in the peak concentrations of the plume lying towards the edge of the array, or on occasions missing it altogether.

To clarify the situation the analysis was begun by drawing a scale diagram for each experiment, in order to estimate the angle of the axis of the receptor array to the mean flow, with particular reference to the peak in the crosswind profile of concentration. It will be observed from figs 5a, 5b that if the distance from the source to the centre of the array, CS, is used to construct a crosswind concentration profile - that is, assuming an arc of equidistant points PCQ rather than attempting to use the different distances AS, CS, BS - then two effects arise due to any obliquity of the array axis: (i) the apparent width of the array as viewed from the source is reduced and (ii) the distance of the off-centre samplers such as A, B, from the source is either over- or under-estimated. The two effects are not strictly additive but may be partially compensating depending on the geometry. An important consideration is the location of the peak concentration with respect to the array, as a given percentage error near the peak will have a greater effect when determining the profile than a similar percentage error in the 'tail'. A correction for the difference in angle subtended at the source, bias (i), can be made quite easily if necessary, by weighting σ_y by $\sin\theta$. There is no

straightforward adjustment for bias (ii) which may be ignored with reasonable safety only if it can be offset against a bias (i) effect and the position of the peak concentration is favourable. As a result of this preliminary investigation data from only 4 runs were retained as likely to provide useful information on the crosswind dispersion - Exps. 2, 3, 8 and 9, with fig 5a-type geometry. Experiments with a fig. 5b geometry were rejected.

7. Method of Analysis

Initially the vertical levels of the array were situated at 0.7, 4, 8, 11.5 and 15m above the hill surface. This was altered to 0.7, 4, 8 and 10m for runs 7 to 9. A wind profile was computed for each of the acceptable runs using 2m observations taken on site at the time of the experiment, together with plotted isotachs of the mean hourly 8m wind over Blashaval. The latter were derived from measurements compiled throughout the primary mean flow/turbulence experiment in progress at the time (MK85).

The estimates of wind direction were used in conjunction with the dispersion data to fix the location of the peak concentrations as accurately as possible. Cross-wind concentration profiles were then constructed by joining the observations across the width of the plume with a smooth curve, and σ_y computed. For many cases only a half-width of the plume was intercepted, and σ_y was estimated as the root-mean-square distance from the peak profile.

Owing to the demands made by the main Blashaval experiments upon the available equipment, it was not possible to make direct readings of the turbulence at the point of release. However, in addition to the hourly logging of the mean 8m wind the standard deviation of its direction (σ_θ) was recorded at a number of sites throughout the period of experiment, and

turbulence data were collected for the 'upstream' and 'summit' sites on many occasions (full details are to be found in MK85). As, to a first approximation, σ_θ can be taken as representative of lateral turbulent intensity

$$\bar{u}\sigma_\theta \simeq \sigma_v ,$$

the records of the upstream mean flow and standard deviation could be used to identify turbulence regimes (from those available) most nearly corresponding to those obtaining at the time of the dispersion experiments. The upstream or summit measurements of σ_v for these regimes were thus available for rough comparisons with the estimates from the dispersion data. For the upstream turbulence observations, the σ_v were usually fairly constant in the vertical, and averaged figures were used for comparison with the 8m slope estimates.

A ratio similar to (8) may seem to be the obvious one for comparing upstream and slope turbulence, but the fact that only dispersion data are available for the slope estimates makes it inappropriate. This is because the dispersion will include components due to horizontal divergence. Accordingly (8) is replaced for mid-slope by a corresponding ratio of crosswind dispersions, weighted by the mean wind strengths:

$$D(\text{slope}) = \frac{\frac{\bar{u}^2(\text{slope})}{\bar{u}_\infty^2}\sigma_y^2(\text{slope}) - \sigma_{y,\infty}^2}{\sigma_{y,\infty}^2} \qquad (9)$$

using $\sigma_{y,\infty} = \sigma_{v,\infty}(\tau, T/\beta)X/\bar{u}_\infty$, where X is the distance travelled. β

was obtained from βi = 0.6, which PS83 consider preferable to the earlier estimate of 0.44, and gives values of D(slope) of slightly lesser magnitude. The subscript ∞ refers to the upstream value, and the slope and upstream values of σ_y are estimated over the same distance. D(summit) is similarly defined, and will have identical theoretical magnitudes to summit values of $\Delta\sigma_v^2(\tau, T/\beta) / \sigma_{v,\infty}^2(\tau, T/\beta)$. The ratio (9), however, avoids unwarranted implications as to the mechanism of the crosswind motions.

The plume width is defined as the distance between the points at which the concentration falls to $1/10$ of the peak value, and was estimated from the profiles. The ratio of the plume width to σ_y is 4.29 for a Gaussian plume. In the present context, for a given σ_y and peak concentration, a ratio smaller than 4.29 implies a concentration profile which is "top heavy" in comparison with the Gaussian, and a ratio in excess of 4.29 a profile which tends to be rather more 'spiked', or thicker-tailed. The ratio is quite sensitive to the geometry of the tail.

8. Experimental Results (crosswind dispersion)

8.1 Exp 2 For this experiment, 0.85 litres of tracer were released over 20 minutes. A scaled plan along the lines of fig 5 revealed that the biasses, (i) and (ii), were small and mutually compensating, while the peak concentration seemed very well positioned. The centre-line CS lay along 165° magnetic, the receptors along 263°, the measured 2m wind at the point of release was 178°/4.4 msec^{-1}, and the estimated 8m wind approximately 170°/6.0 msec^{-1}. From these figures one would expect the peak to fall just within the eastern edge of the array, and this is supported by the dispersion data (which were close to Gaussian). The possibility exists that the peak, nonetheless, lay just outside the eastern edge, but the

consistency of the dispersion figures, and of the ratios of plume width to σ_y (about 4.3 to 4.6 in the range 4-11.5 metres) offer little support for the likelihood of a significantly exaggerated estimate of the dispersion, which is possible if a fairly sharp peak is just missed. For broad Gaussian peaks, a receptor array which just fails to intercept the maximum concentration values will tend to yield a plume width to σ_y ratio < 4.29. The mean flow distortion conditions at Blashaval (section 8.2) suggest that broad peaks would be the more likely for Exps. 2, 3 and 8. If this is the case, ratios of 4.3 to 4.6 suggest that the σ_y measured in Exp. 2 may even be on the conservative side.

The Table of Results (Table 3) shows that at 109m the plume width at a height of 8m was about 78m. This is nearly double the average of about 40m for a 100m traversal quoted by PS83 for a ground level source over level grassland. The ratio D(slope) computed using the best available upstream turbulence data was 2.63. D(summit) has a theoretical value of around 1.7; for a flow which was still accelerating a D-ratio 8m above the surface may be expected to be well below that figure. It would seem that a substantial part of the crosswind spread must be attributed to the non-turbulent effects outlined in section 6, in particular the lateral divergence.

8.2 Exp 3 The set-up for this experiment is identical to that of Exp 2 except that the winds were veered a few degrees and a little stronger. The more southerly wind direction puts the peak concentration perilously close to the eastern edge of the array. The dosages absorbed from a release of 1.4 litres over 14 minutes were small (section 3) and the distinct possibility exists that at some levels the peak lay just outside the eastern edge of the sampler array - this despite a recorded observation that the spray initially set off "right down the centre-line". The 8m flow

estimated from isotachs was 175°/8m sec^{-1}, close to the centre-line, but for this experiment no 2m observation was available at the point of release. Despite the low dosages the 4m and 11.5m dispersion data give a good approximation to Gaussian with a profile peak just inside the array while at 0.7m and 8m the peak was assessed to lie at the easternmost edge. If however, the peak was just missed, then the plume width is probably underestimated and (in view of the ratio of plume width to σ_y, 4.13) unlikely to be seriously overestimated.

The ratio D(slope) estimated at 2.56 for this experiment, is similar to that for Exp 2, again well in excess of the summit ratio (8). It is possible to make an approximate estimate of the contribution of lateral divergence to the spread of the plume using the observed 8m wind field at the time of the experiment in conjunction with a plot of the distortions imposed upon the mean flow by the hill computed using a Jackson and Hunt model. A 3-dimensional version of the model was developed by Mason and Sykes (1979). Further development of the model and a comparison of the modelled and observed flows over Blashaval may be found in MK85. The version used in this paper is 'Model C' as described in MK85. Divergence was not taken directly from the Jackson and Hunt results as the model tended to under-estimate the lateral perturbation. (It was later found that the Model C wind component perturbations are considerably smaller than those obtained using a revised version (Model D), considered more realistic). For Exp 2, for instance, the maximum diffluence over the windward slope estimated from Model C (fig 6) is about 16°, while the corresponding observation is not below 25°. In addition, there is some difficulty in precisely locating the experimental sites on the model output.

In view of these considerations the Jackson-Hunt model was used only to estimate the ratio of the divergence over the area of the experiments to the mean divergence between the zones of maximum deflection of the wind. These zones are then located on the plots of wind observations, and the divergence of the plume due to mean flow distortion estimated using the observed large-scale diffluence of the mean flow and the ratio estimated from the model. In effect, the Jackson-Hunt computation is used to add the necessary resolution to the observed wind pattern.

When a representative mean transverse divergence, div_y has been obtained it is a simple matter to estimate a notional plume width net of divergence, Y, from

$$Y = W - \iint div_y \, dy dt \qquad (10)$$

Here, W is the measured plume width, and it is assumed that, to a first approximation, the components due to lateral divergence and turbulent motion are additive. Assuming further that this notional plume (ie. excluding divergence effects) is Gaussian, a revised estimate of σ_y is immediately obtained and D(slope), now roughly equivalent to the slope value of (8) recomputed. This ratio is distinguished D_t(slope), the subscript t implying a restriction to turbulent spread.

For Exps 2 and 3 the ratio of site to large-scale mean divergence was estimated to be near 2, from which

	Increase in plume width due to divergence (m)	D_t(slope)	
Exp 2	17.1	1.26	} (11)
Exp 3	19.8	1.31	

In estimating the diffluence of the broad scale flow it was noted that compared to Exp 2, the winds of Exp 3 were veered by rather less than 5° (on average) on the western upwind flank of the hill, and well over 10° (on average) over the eastern upwind flank and summit. It was deduced that lateral divergence was slightly greater in the case of Exp 3, possibly due to the closer approach of the southerly (veered) wind to complete perpendicularity with the hill contours around the experimental site.

The values of D_t(slope) at (11) should be compared to the theoretical summit value of about 1.7. Indeed, if the relative accelerations for the two runs are taken into account it is found that

	$\frac{D_t(\text{slope})}{D(\text{summit})}$	$\frac{\bar{u}(\text{slope})}{\bar{u}(\text{summit})}$	
	%	%	
Exp 2	70	82.1	} (12)
Exp 3	72	74.8	

Taking the ratio between columns as roughly equal to unity it may be deduced that the (dimensional) increment $\Delta\sigma_v^2 / \bar{u}$(local) was approximately the same for the slope (below and up to site A) and summit or, more generally, assuming that the approximations made have not led to serious error, that the dimensionless increase in crosswind turbulent energy $\Delta\sigma_v^2 / \bar{u}^2$(local) was about 25% greater at the slope location than

on the summit. This increase may be due in part to the convergence of streamlines in the vertical above the slope, which may possibly contribute to increased diffusivity (section 13).

The figures suggest that despite the uncertainties associated with the experiments a fair level of consistency was in evidence both between the experiments and with the indications of the broad scale flow. These experiments allow, perhaps, a first approximate quantification of the relative effect upon dispersion of mean flow distortion and increased turbulence on the middle slope of an isolated hill.

8.3 Exp 8 For Exps 7-9 the experimental site was moved upslope, and lay quite close (within about 150m) of the summit (see Fig 2). The sampler array was aligned at approximately 270° magnetic and with the centre line for Exp. 8 at 163° there was slightly more obliquity than in Exps 2 and 3. The 2m wind measured at source was 159°/11.2 $msec^{-1}$ and the estimated 8m flow about 160°/15 $msec^{-1}$. The wind direction implies that the concentration peak should reach the sampler array just to the left (west) of the centre-line. The dispersion data, however, show that much of the tracer was steered onto the eastern half of the array, accordingly providing an acceptable fig 5a-type geometry. On this occasion 1.7 litres of tracer were released over 10 minutes, and the quantities of tracer absorbed were large: apparently excessively so at 0.7m. It is apparent, however, that much of the tracer is being forced towards the hill surface. The crosswind profiles are irregular, with the peaks variously located at the different levels. In view of the convergence and depression of the vertical streamlines it was decided to confine attention to the 4m data - at this level concentrations were quite large and roughly Gaussian, while at 0.7m the horizontal profile is incomplete and the extraordinarily large

figures may indicate contamination or some near-surface complication. The notional upstrem dispersion was still computed for 8m. Summit turbulence readings were available for this run, but unfortunately no close upstream parallel could be found. The upstream turbulence can be approximated from the summit readings if the theoretical maximum of D(summit) = 1.7 is assumed to apply. Using the 3m summit reading this assumption yields $\sigma_{v,\infty} \simeq 0.77$. For the best available upstream readings $\bar{u}\,\sigma_\theta$ exceeded the corresponding values for Exp 8 by 50%. If, as a rough check, the corresponding upstream turbulence measurement is reduced proportionately an estimate $\sigma_v \simeq 0.74$ is obtained, which is reasonably close. The upstream turbulence intensity $(\sigma_{v,\infty}/\bar{u})$ of the other experiments was close to 0.1; this figure yields $\sigma_{v,\infty} \simeq .92$ for Exp. 8, and is adopted here as it gives the most conservative value for D(slope).

At 4m the ratio of plume width (78m) to σ_y (18.8m) is 4.1, which is comparable to Exp 3. The dispersion ratio D(slope) is 5.95 which seems excessive. However, the release of tracer for Exp 8 was made in the zone of maximum horizontal divergence near to the line, incidentally, along which the sign of the forced lateral deflections changes. The ratio of the modelled mean site divergence to the large scale value is estimated at around 2 to 2.5, while local effects beyond the resolution and scope of the smoothed linear model may have contributed to the spread. A ratio of 2 would correspond to a divergence-induced increase in plume-width of about 22m and a value of D_t(slope) around 2.37. This is well in excess of the theoretical summit value (1.7). The ratio of 2.5 yields D_t(slope) about 1.9, near the theoretical limit, with an increase in plume-width of about 25.5m.

If the estimates for Exp 8 at 4m are to be acknowledged as giving even a qualitative indication of the spread, the large ratio D_t must be accounted for. Apart from inadequacies of the model or samplers or the possibility that the broad-scale divergence has been underestimated from such observations as are available, it can only be suggested that low-frequency meandering of the wind may have been enhanced by the presence of the hill, thus boosting σ_v(slope). There was little evidence for this effect with the lighter winds of the mid-slope Exps 2 and 3, but the forcing may have been less rigid on the upper slopes. Certainly the relatively much stronger winds of Exp 8 should not exaggerate the mean flow distortion, as high Reynold's number flows exhibit dynamical similarity - in neutral conditions the turbulent Reynold's number

$$R_t = \frac{\bar{u} L}{K_m} = \text{constant}$$

(Km is eddy diffusivity).

Exp 8 fails to provide a firm enough foundation for any strong conclusions. The tracer was, however, released at about the position of maximum lateral divergence and taken with runs 2 and 3 the experiment underlines the major role of mean flow distortion in influencing the spread of pollutants from a low level source on the windward slopes of a hill. These effects may vary quite rapidly with height above the hill surface.

8.4 In Exp 9 1.5 litres of tracer were released over 10 minutes, and again large quantities were absorbed by the passive samplers. The site of the experiment was unchanged from Exp 8, but as the wind had veered to SSW the point of release was moved. The centre-line was now 220° magnetic; the 2m wind near the source was measured as 233°/13.6 $msec^{-1}$. The broad-scale 8m wind however could not have been much further round than

210°, with a speed estimated at no less than 17m sec^{-1} - testing conditions in which to carry out a dispersion experiment. Fortunately there is little doubt that the peak concentration was fairly central by the time the plume reached the sampler array.

The scaled plan is of the fig 5b type with biasses (i) and (ii) both tending to exaggerate the estimates of dispersion: the angle between the centre-line and the axis of the sampler array was no greater than 50°. Nonetheless, useful results could be obtained in this case - as the peak concentration was fairly central, the bias (ii) error was not serious, whereas the bias (i) error could be corrected (approximately) using a weighting of sin 50°, that is, about 0.77. Qualitatively similar results were obtained even omitting this adjustment.

Considerably less tracer was absorbed at 0.7m than at higher levels, suggesting that the plume was not being forced towards the surface as in Exp 8. At 4m estimates of dispersion are very approximate, owing to the skewness of the profile. The ratio of plume width to σ_y, 4.4 at 8m reflects a small σ_y rather than a wide plume. The plumes were, in fact, very narrow - little over 30m after the bias (i) adjustment. The dispersion ratios, D(slope), are at 0.02 and 0.18 for the two levels clearly in a completely different category from Exp 8. Even omitting the bias (i) adjustment D(slope) is 0.72 and 1.03 respectively. Evidently, σ_y is reduced in comparison to the upstream values, and the most likely mechanism for this effect is lateral convergence rather than divergence. The explanation for this lies in the different wind direction, which in effect 'shifts' the array towards the right-hand shoulder of the hill (looking downwind). The evidence of the dispersion data is that the flow is converging, transversely, on the right of the hill crest. This effect is not easy to

locate in the observed broad-scale flow with its inadequate resolution, nor in this case, does the Jackson and Hunt computation provide more than qualitative confirmation -careful scrutiny of the model output suggests that the tracer was released in a zone of weak lateral divergence and was converging weakly by the time it reached the receptor array.

Working backwards from the assumption that D_t(slope) should be fairly close to the theoretical summit maximum - say 1.6, which reflects the magnitude of $\bar{u}$(slope) relative to the summit velocity, and utilizing the observation below (12) - an 8m σ_y of 12.0 and plume width of 51.6m are obtained. These are notional figures excluding convergence effects. Expression (14) can then be used to obtain $div_y = -0.06$ sec^{-1}, a convergence of only slightly lesser magnitude than the more extreme of the estimates of the divergence in the calculations of D_t for Exp 8.

9. Divergence and Flux

The flux F_c, of a contaminant is conventionally represented by a flux-gradient relationship such as

$$F_c = -\rho K_c \frac{\partial \bar{c}}{\partial n}$$

where $\partial \bar{c}/\partial n$ is the concentration gradient perpendicular to the streamlines and K_c a crosswind eddy diffusivity for the contaminant. As Hunt et al (1983) point out, if a plume is embedded in converging streamlines the tightening gradient will result in fluid elements crossing the streamlines more rapidly. The turbulent dispersion accordingly increases, and the effect of the convergence in reducing the rate of spread is reduced with distance downwind. Similarly the rate of spread of a plume may be progressively reduced with downwind distance if the streamlines diverge. The implication is that the components of the plume spread

attributable to turbulence and convergence/divergence at a given distance from the source are not additive, but are related in a way which depends upon the history of the plume.

For airflow over a hill horizontal divergence is not associated with a reduction in u_* (and hence K_c) - indeed, the air will be accelerating up the hill, and there will be no tendency for the plume spread to be inhibited. For Exp. 9 divergence of streamlines in the vertical presumably tended to offset any acceleration due to convergence in the horizontal, although u_* may have been slightly increased along the trajectory by the normal upslope acceleration. In the present analyses any inaccuracies due to the absence of strict additivity of dispersions due to turbulent and mean motions are probably outweighed by the various approximations and sampling effects.

10. Vertical dispersion: introduction

There is a fundamental difference between horizontal and vertical motions close to the surface in that the low-frequency horizontal oscillations are largely absent from the vertical. This makes little difference to most theoretical approaches to dispersion since low frequency oscillations are either effectively ignored, or if the wavelength is not too long, treated as a component of the turbulence structure. PS83 outline three regions of dispersion from an elevated source:

(i) A region close to the source where no material has reached the ground level.

(ii) Long range, where the ground level concentration is decreasing with the horizontal distance, X, and the profiles are tending towards those for a surface release.

(iii) The intermediate range, after material first appears at ground level. Here, the dispersion cannot be described in terms of the classical statistical theory because of the variation of the turbulence structure with height. The present experiments fall within this category.

Vertical dispersion from surface releases has been analysed by extending the classical theory (Hunt and Weber, 1979) and more empirically, by determining 'shape exponents' to fit the profiles. For elevated sources the Gaussian plume has often been adapted (for practical purposes) but it is more appropriately restricted to case (i) above. In the following sections the observed Blashaval concentration profiles will be examined in the light of a solution of the diffusion equation and of simulations using a stochastic technique - the random walk dispersion model.

11. Vertical dispersion on an upwind slope

11.1 Over level ground the equation of diffusion can be solved analytically provided the profiles of wind strength and eddy diffusivity are specified in a suitable manner. Smith (1957) obtained very reasonable results by assuming a power law:

$$\left.\begin{aligned} \bar{u}(z) &= \bar{u}_c z^{\gamma} \\ K(z) &= K_0 z^{1-\gamma} \end{aligned}\right\} \qquad (13)$$

where $\gamma = 1/7$ for neutral conditions and $K_0 = ku_*$, numerically. The profile is given by

$$C(X,z) = \frac{(zz_s + z_s^2)^{\gamma/2}}{(1+2\gamma)K_c X} \exp\left[\frac{-\bar{u}_c (z+z_s)^{1+2\gamma} + \bar{u}_c z_s^{1+2\gamma}}{K_0 (2\gamma+1)^2 X}\right]$$

$$\times I_{-\frac{\gamma}{1+2\gamma}}\left[\frac{2\bar{u}_c (zz_s + z_s^2)^{(1+2\gamma)/2}}{K_0 (2\gamma+1)^2 X}\right] \qquad (14)$$

where C(x,z) is a normalised concentration, $I_{-\frac{\gamma}{1+2\gamma}}$ a modified Bessel function. This solution is for an elevated line source but may be taken as appropriate for the concentration at the peak of the crosswind profile. Although the mean vertical displacement of a puff over horizontal terrain quickly becomes positive, i.e. rises as X increases, the mean Eulerian displacement changes only slowly with X, while the concentration peak sinks slowly. These effects are due to the profiles (13). Formula (14) is adequate for establishing a reference profile over level terrain but for the differences brought about by the distortion of the mean flow due to the presence of a hill the most practicable technique is random walk modelling.

11.2 An account of the rationale and practical formulation of the random walk modelling of dispersion based upon the Langevin equation and the Markov process is given in Ley and Thomson (1983) and Thomson (1984a). Thomson has adapted his standard random walk formulae to take account of non-zero mean initial motions. The formulation used simulates the vertical motions of a large number of particles released at the source, and advects them with the local horizontal airflow:

$$w_{i+1} = \alpha w_i + (1-\alpha^2)^{1/2} \sigma_w \eta + \frac{\Delta T}{t_L} \bar{w} + \Delta T \frac{\partial \bar{w}}{\partial z} \cdot w_i \qquad (15)$$

This excludes, for economy's sake, along-wind dispersion which made little difference to the vertical concentration profiles. In (15),

w_i, w_{i+1} are the instantaneous vertical velocities of a particle at timesteps i, i+1

$$\alpha = \exp\left(-\frac{\Delta T}{t_L}\right)$$

η is a normally distributed N(0,1) random variable

σ_w is estimated at $1.3\, u_*$

t_L the Lagrangian time scale is estimated from $\frac{k u_* z}{\sigma_w^2}$

The last two terms in (15) take account of the profile of mean vertical velocity, which for simplicity was given a constant value

$$\frac{\partial \bar{w}}{\partial z} = -\overline{\left(\frac{\partial \bar{u}}{\partial x} + \frac{\partial \bar{v}}{\partial y}\right)} \simeq -\left(\frac{\partial \bar{U}}{\partial x} + \frac{\partial \bar{V}}{\partial y}\right) \qquad (16)$$

where the long overbar and $\bar{U}, \bar{V}$ are averages through the depth of the slab. In justification, plotted Jackson and Hunt results suggest that the vertical velocity profile is approximately linear below about 10m.

The mean divergences were estimated as accurately as possible from the observed wind field and the ratio of high- to low-resolution divergence determined from runs of the Jackson and Hunt model, as described in section 8.2. The plotted sample Jackson and Hunt profiles showed that the mean velocity perturbation for the slab below 8m was closely approximated by the 8m magnitude, which was accordingly used in (16). The mean winds below 8m, also required for (16), are easily calculated for neutral conditions by integrating the log profile:

$$\bar{U} = \frac{1}{z}\int_{z_0}^{z} \bar{u}(z)\, dz = \frac{u_*}{k}\left(\log_e \frac{z}{z_0} - 1\right) \qquad (17)$$

12. Vertical dispersion - experimental results

12.1 As the vertical profile of concentration is not sensitive to the angle between the wind and the receptor array, Runs 2-9 were all examined. The eight runs can be broken down into five categories, depending upon the position of the experiment and the wind direction:

Experimental Site	Wind regime S-SE	SSW-WSW	
A (mid-slope)	2, 3	-	
B (")	6	4,5	Experiments
C (near-crest)	7, 8	9	

Figure 7 shows for each category the vertical profiles expressed as percentages of the total tracer absorbed in the column of receptors nearest the peak concentration. The irregular but broadly elliptical cross-section of the plume excludes from consideration the vertical profiles at any distance from the peak. In one or two cases, to be discussed, the peak vertical profile looks anomalous, and adjacent profiles will be scrutinised. Each experiment was simulated using the random walk model (15) for which u_* was estimated from the local wind and a mean vertical velocity estimated and incorporated as described in section 11.2. For each experiment the motions of 7000 passive 'particles' were simulated, and a vertical profile of concentration computed at the appropriate distances downwind. These profiles are also plotted in fig 7 together with the reference level terrain profiles computed more economically using (14).

In all the experiments the 0.7m dosage considerably exceeds that of the level terrain reference (computed, as in the case of the random walk, at 1m for convenience). This may be due in part to the conditions of the experiment (retention and slow release of tracer by vegetation for

instance), a possibility which must be borne in mind when comparing the observed profiles with the reference and simulated ones. In part, however, it is no doubt due to the equilibrium profile of mean vertical velocity.

12.2 Exps 4 and 5 With the wind from the SW'ly quarter the experimental site for Exps 4 and 5 was effectively on a flank of the hill. These profiles (fig 7c) show the closest approach to the level terrain solution, and suggest that the net divergence effects were slight. Off-centre divergence proved to be particularly difficult to quantify from the observed winds and Jackson-Hunt model, nonetheless an estimate ($-.037\ sec^{-1}$ presumably excessive) was made and Exp 4 simulated; the profile is reproduced in the figure for comparison with the other simulations where the divergence was stronger.

12.3 Exps 2 and 3 These profiles are the most surprising having the appearance of dispersion profiles at much greater downwind distances than the 109m of the trajectory. On the plotted profiles (fig 7a) the peak concentration has descended to the surface and there is no apparent convexity between the surface and the 8m release height. The impression is given that steady downward mean vertical motions were combined with marked turbulent spread. For Exp 2 a second vertical profile (with rather more tracer content than that plotted) exhibits a peak at 11.5m. This is inexplicable except in terms of an oddity in the local flow or as a random effect. Like those plotted, however, and other profiles from Exps 2 and 3, it displays a uniformly high level of vertical dispersion (Table 1).

The marked vertical spread must be largely due to the σ_w^2 profile, which was observed by MK85 to increase with height over the summit of Blashaval. They attribute this effect to the transition towards rapid distortion conditions above a height of $L/2\pi$. No doubt a weaker

effect is operative on the mid-slopes of the hill unless the mean vertical motion is large enough to depress the plume strongly. It is possible that, despite the Jackson and Hunt indications, the mean vertical velocity gradient increases close to the surface as a consequence of the turbulence field (section 13) so that downward advection outweighs other effects near the ground. The concentration profiles of Exps 2 and 3 appear to exhibit the combined effects of the turbulence and vertical velocity structures.

The random walk simulations again suggest that the estimated vertical velocities were excessive. The velocities are, however, reasonably well supported by the horizontal dispersion analyses while the simple mean vertical velocity prescription and turbulent parametrization of the random walk could take no account of effects such as those suggested.

12.4 Exp 6 This experiment was conducted at the same site as Exps 4 and 5. It differs in the strength and direction of the wind which was east of south and at gale force. In this case the plume was evidently forced strongly towards the hill surface, and is well simulated by the random walk. Indeed, the observed profile (fig 7b) can be reproduced almost exactly if a slightly larger vertical velocity is assumed. In contrast to Exps 2-5, the vertical velocity, although the largest calculated $\left(\frac{\partial \bar{w}}{\partial z} \simeq -0.103\ s^{-1}\right)$, appears to have been marginally underestimated, unless near-surface modification as suggested in the previous section is contributing to the plume depression. The inadequacy of the reference level terrain solution, and the apparent success of the random walk simulation, are pronounced.

For this experiment a longer range random walk simulation was made with Eulerian concentration profiles estimated up to $x/z_s \sim 125$ downwind (fig 8). The curves show that the plume descends quickly at first, but the

mean height levels out at $z/z_s \simeq 0.54$. The maximum concentration reaches the surface at $x/z_s \simeq 15$, and remains there. In reality the surface concentration must steadily decrease, but in a two-dimensional model the process is very slow in the presence of mean downward motion.

12.5 Exps 7 and 8 Two further strong wind experiments but now located at site C, nearer the hill crest (see fig 2). The vertical array was shortened to 10m for site C, but both Exps 7 and 8 display a very strong forcing towards the surface. Indeed, in fig 7e a flank profile has also been plotted for Exp 8 as the near-peak profiles were almost entirely concentrated at 0.7m. Given that the 0.7m concentrations are spurious, it must still be recalled that the analysis of the Exp 8 4m crosswind spread also indicated extremely strong divergent motion. It seems likely that the situation of the tracer release point in the zone of maximum mean flow distortion is material in the development of extreme profiles, since plume depression can occur before significant vertical spread due to turbulence has time to develop. For Exp 7, the plume centroid seems to have missed the receptor array, and the curve plotted (fig 7d) is presumably a flank profile. The indications are again of marked downward mean motion, which would very likely have been more in evidence in a peak profile.

The random walk simulations are reasonable for the two flank profiles, and certainly very superior to the reference level terrain curves. If the peak Exp 8 profile is representative, it is quite certain that important but unknown factors or quantities have been omitted from the simulation.

12.6 Exp 9 As has been noted, this experiment was unique in the series in that significant convergent as well as divergent motions seem to have been involved. Indeed, the Jackson-Hunt model implies that the release took place in a zone of divergence, but that the plume was quickly deflected

into a region of convergence. It is unlikely that the random walk prescription of a net, weak mean upward vertical velocity would reproduce the vertical concentration profiles very accurately, but it will be noted (fig 7f) that one of the two profiles plotted was simulated quite well. The other profile seems suspect in any case.

The observed column 4 profile (see Table 1) appears to reflect the complicated history of the plume with the peak held near 8m apparently due to a balance of the various forcings (vertical profile of diffusivity and wind, mean upward vertical motion due to lateral convergence) but cutting off sharply above, perhaps as a result of an earlier history of divergence and downward motion. Alternatively (and speculatively) the profile may in part result from a combination of along-wind divergence coupled with cross-wind convergence, or a change in the divergence profile with altitude.

The random walk simulation placed the maximum concentration accurately, for column 4, between 7 and 8 metres above the surface.

13. General Conclusions

These experiments illustrate the many vicissitudes which may befall a plume released on the upwind slope of a hill, even in neutral conditions. On the mid to upper central slopes the distortion of the mean airflow by the hill will stretch the plume along- and across-wind, so that a resultant mean vertical motion forces the plume towards the surface. If the depression is not too strong some of the material may experience a more rapid dispersion in the vertical as it reaches levels of stronger σ_w^2, which increases with height above the surface as the air is lifted towards the summit. On the shoulders of the hill the plume may encounter areas of crosswind convergence which it seems may become quite strong where the

shape of the hill is irregular or asymmetric. The dispersion profiles are thus site-dependent, to a marked degree, while any particular plume may, even over a few score metres, move from one regime of mean flow perturbation into another. It is quite possible for a plume to be significantly deflected over a trajectory of 100m, a fact which can add to the difficulty of arranging a successful dispersion experiment. Fig 9 illustrates this point. It reproduces wind-component fields from the Jackson-Hunt model corresponding to Exp 4, and shows how the plume, released from a point to the left of the summit and below the centre-line as marked in the diagram, will be steadily turned to the left on the upwind slope. On the other hand the Exp 2 plume (Fig 6) released to the left of the summit and above the centre-line of the diagram, would be deflected to the right. It will be observed from these diagrams that even over the summit a perturbation occurs, which is in the opposite sense for the SSE'ly Exp 2 to the WSW'ly Exp 4. The 8m wind observations confirm these perturbations, at least qualitatively.

The increase in dimensionless crosswind turbulent energy $\Delta\sigma_v^2/\bar{u}^2(\text{local})$ appeared to be about 25% greater on the windward mid-slope (below site A) than over the summit. This effect (which the various approximations may have exaggerated) may be helped, it is speculated, by an increase in diffusivity associated with the presence of a gradient of the mean

velocity perpendicular to the slope. The vertical concentration profiles of the moderate wind experiments 2 and 3 give the impression of a transition with height above surface. Close to the ground the mean vertical velocity profile, which reflects the turbulent energy/mean flow distortion equilibrium associated with the form drag, may be relatively sharp, helping to confine the plume; at higher levels turbulent spread assumes greater relative importance as σ_w increases towards the 'rapid distortion' levels. All of these suggestions are discussed in more detail in Maryon, 1984. For the strong wind case, Exp. 8, the equilibrium mean perpendicular velocity seems to assume greater relative importance — downward advection predominates. The crucial factor is presumably the site rather than the wind strength. If Exp. 8 is accepted as providing qualitative information it seems that where a source is situated in a region of strong divergence the plume is rapidly depressed before turbulent vertical spread becomes significant.

The downward advection explains part of the high concentrations observed at 0.7m. Observational validation or quantification from the present experimental results is difficult, however, since the vegetation cover may have retarded dispersion of the tracer and to some extent biassed the readings at the lowest level. Instrumental verification of the three-dimensional velocity structure is desirable.

The plume of Exp 9 provided evidence of a complicated history. In this case an area of strong lateral convergence seems to have been reached and traversed, with the resultant σ_y falling well below level terrain values. Finally the possibility of vertical shear being imposed upon the plume by the change in the magnitude of the mean flow perturbations with

height must also be borne in mind. This effect has not been investigated here, but must add to the complication of the plume cross-section as is evident in many of the results.

The results of simulations 2, 6, 8 and 9 suggest that the random walk technique for modelling dispersion has considerable potential for adaptation to complex terrain provided the pattern of distortion is not too complicated. The simulations displayed a greater family likeness than the actual dispersion data, and were obviously constrained by the very basic mean flow and turbulence parametrization. No doubt more flexible models might be developed which may prove to be of practical use, but a number of problems remain to be solved. The upslope acceleration, the other perturbations to the mean flow and their changes downstream and with elevation must be prescribed with sufficient resolution and somehow incorporated into the model. Progress may be made by running the random walk in association with suitable numerical models predicting the mean flow (for example, Thomson, 1984b). Slope turbulence structures need to be better understood and the parametrization reviewed, while the difficulties posed by low frequency horizontal fluctuations remain.

In this analysis an attempt has been made to extract signal from a few realizations of what must be highly variable situations. Further experiments are required to establish which of the results is repeatable. Adequate on-site instrumentation is essential, and would obviate the extensive estimation and approximation (eg. of turbulent intensity and divergence) which have been resorted to in this initial investigation.

Acknowledgements

The authors would like to acknowledge their debt to the staff of the Met Office Boundary Layer Branch based at Bracknell and Cardington who conducted the North Uist field experiments under what were often extremely difficult and unpleasant conditions. A. Gould of C.D.E., Porton Down, Salisbury was, with G J Jenkins and J. B. G. Whitlock, mainly responsible for the design and execution of the dispersion experiments. A. Gould and P. A. Hollingdale-Smith, also of C.D.E, provided and analysed the chemical samplers. We are grateful to a number of the staff of the Boundary Layer Branch for interesting discussions - particularly D. J. Thomson who, in addition, carried out the random walk simulations.

References

Bailey A. and Hollingdale-Smith, P. A. 1977. A personal diffusion sampler for evaluating time weighted exposure to organic gases and vapours. Ann. Occup. Hyg. vol 20, p 345.

Britter R. E, Hunt J.C. R. and Richards, K.J. 1981 Airflow over a two-dimensional hill: studies of velocity speed-up, roughness effects and turbulence. Quart. J.R. Met. Soc 107 p.91.

Hay J.S. and Pasquill F., 1959. Diffusion from a continuous source in relation to the spectrum and scale of turbulence. Atmospheric Diffusion and Air Pollution ed. F. N. Frenkiel and P. A. Sheppard, Advances in Geophysics 6 p.345, Academic Press.

Hunt J.C.R. and Weber A.H. 1979. A Lagrangian statistical analysis of diffusion from a ground level source in a turbulent boundary layer. Quart. J.R. Met. Soc. 105 p.423.

Hunt J.C.R., Puttock J.S. and Snyder W.H. 1979. Turbulent diffusion from a point source in stratified and neutral flows around a three-dimensional hill - Part I. Diffusion equation analysis. Atmospheric Environment 13, 9, p.1227.

Hunt J.C.R, Leibovich S., and Lumley J.L. 1983. Prediction methods for the dispersal of atmospheric pollutants in complex terrain. Final Report to State of Maryland Dept. Nat. Res. Contract No. P85-81-04.

Jackson P.S. and Hunt J.C.R. 1975. Turbulent wind flow over a low hill. Quart J.R. Met. Soc. 101 p.929.

Ley A.J. and Thomson D.J. 1983. A random walk model of dispersion in the diabatic surface layer. Quart J.R. Met. Soc. 109 p.867.

Maryon R.H. 1984. Lagrangian plume development in a gradient of imposed mean vertical motion. Met Office Turbulence and Diffusion note No 167.

Mason P.J. and King J.C. 1985. Measurements and predictions of flow and turbulence over an isolated hill of moderate slope. Quart. J.R. Met. Soc, to appear in April issue.

Mason P.J. and Sykes R.I. 1979. Flow over an isolated hill of moderate slope. Quart. J.R. Met. Soc. 105 p.383.

Pasquill F. and Smith F.B. 1983. Atmospheric Diffusion, 3rd Edition. Ellis Horwood Ltd, Chichester.

Smith F.B. 1957. The diffusion of smoke from a continuous elevated point-source into a turbulent atmosphere. Jnl. Fl. Mech., Vol 2, Part 1, p.49.

Smith F.B. 1973. A scheme for estimating the vertical dispersion of a plume from a source near ground level. Met. Office, Turbulence and Diffusion Note No. 40.

Thomson D.J. 1984a. Random walk modelling of diffusion in inhomogeneous turbulence. Quart J.R. Met. Soc. 110 p. 1107.

Thomson D.J. 1984b. A random walk model of dispersion in turbulent flows and its application to dispersion in the Sirhowy Valley. In preparation.

TABLE 1 BLASHAVAL DISPERSION EXPERIMENTS: MEASURED DOSAGES IN NANOGRAMS

	Column (West-East)	1	2	3	4	5		1	2	3	4	5
	Horizontal Distance (M)	25	12.5	0	12.5	25		25	12.5	0	12.5	25
	Height (M)											
EXP. 2	15	2	25	51	112	119	EXP. 3	1	2	109	67	147
	11.5	0	28	90	124	364		0	9	48	145	157
	8	9	29	98	191	208		1	19	86	99	165
	4	2	31	77	239	219		0	28	59	201	190
	0.7	2	13	40	334	269		0	4	50	97	223
EXP. 4	15	[illegible]	169	178	-	38	EXP. 5	68	110	45	37	60
	11.5	222	194	224	1990	25		5	20	1090	72	111
	8	462	236	188	115	17		51	20	34	140	204
	4	350	236	107	266	124		54	16	80	5430	170
	0.7	355	276	152	24	17		37	86	61	228	192
EXP. 6	15	3	24	12	26	15						
	11.5	4	5	47	249	43						
	8	3	10	61	76	92						
	4	3	14	30	73	245						
	0.7	2	3	14	67	249						
EXP. 7	10	82	4	0	0	0	EXP. 8	10	317	70	94	225
	8	117	18	0	1	0		24	142	997	141	457
	4	117	10	0	0	0		30	272	1077	1060	2110
	0.7	230	5	0	0	0		73	-	1517	11800	9425
EXP. 9	10	0	200	530	300	360						
	8	0	210	1150	1170	200						
	4	0	31	4000	770	650						
	0.7	0	14	450	900	300						

Isolated large dosages, in excess of 1000 nanograms, must be regarded as dubious. There may be an explanation (Section 12.5) for some large dosages close to the surface (Exp 8).

Table 2. Estimates of maximum (centre-line) dosage for experiments 2,3, 8 and 9 assuming Gaussian dispersion over level terrain (see text, section 3). Computations are for X = 100m, z = 8m, height of release = 8m.

Experiment	2	3	8	9
Maximum likely dosage (ng)	812	1016	667	503

SUMMARY OF EXPERIMENTS							HORIZONTAL DISPERSION					TURBULENCE						D - RATIOS (see text)		
EXP	DATE (1983)	TIME (GMT)	VOL. OF SPRAY (litres)	MEASURED 8M WIND (m sec^{-1}) UPSTREAM	SUMMIT	WIND REGIME	HEIGHT ABOVE SURFACE (m)	GAUSSIAN σ_y (m)	DISTANCE RELEASE POINT TO ARRAY CENTRE (METRES)	EST. $\bar{u}(z)$ AT SITE (m sec^{-1})	u_* (m sec^{-1})	EST. PLUME WIDTH (m)	RATIO PLUME WIDTH: σ_y	BEST AVAILABLE UPSTREAM MEASURES HEIGHT ABOVE SURFACE (m)	$\sigma_{v_{-1}}$ (m sec^{-1})	$\sigma_v(\tau, T/\beta)$ (m sec^{-1})	UPSTREAM ESTIMATES USED HEIGHT (m)	$\sigma_v(\tau, T/\beta)$ (m sec^{-1})	EST. $\sigma_{y,\infty}$ (UPSTREAM) (m)	D(SLOPE)	D_T(SLOPE)
2	26/9	1353-1413	0.85	4.5	7.3	SSE	0.7 4 8 11.5 15	10.5 14.0 18.0 16.7 -	109	3.6 5.3 6.0 6.4 -	0.40	37 64 78 71	3.5 4.6 4.3 4.3	3 14	.702 .644	.487 .560	8	0.52	12.6	2.63	1.26
3	27/9	1500-1514	1.4	6.8	10.7	S	0.7 4 8 11.5 15	14.1 14.5 18.6 13.3 -	109	4.7 7.0 8.0 8.4 -	0.53	64 67 77 59	4.5 4.6 4.1 4.4	3 14	.802 .791	.595 .692	8	0.64	10.3	3.51	1.31
4	29/9	1441-1451	1.2	8.4	12.3	WSW	-	-	110		0.72										
5	29/9	1712-1722	0.55	6.0	9.3	SW	-	-	105		0.50										
6	30/9	1012-1027	0.5	13.6	21.8	SSE	-	-	112		1.25										
7	1/10	1554-1604	3.45	11.1	17.3	SSE	-	-	100		1.09										
8	1/10	1733-1743	1.7	9.2	16.0	SE-SSE	0.7 4 8 10	9.7 18.8 -	100	8.6 12.9	0.97	40 78 - -	3.6 4.1	3 14	See text		4	0.92	10.0	5.95	1.9 +
9	2/10	1234-1244	1.5	12.0	18.4	SSW	0.7 4 8 10	7.0* 7.7* 7.3* 13.6*	100	10.1 15.1 17.1 17.7	1.14	30* 31* 32*	4.3 4.0 4.4	5 13	1.304 1.690	1.077 1.521	4 8	1.07 1.24	10.1 10.3	0.02 0.18	- -

* Computed after 'Bias (i)' type correction (see section 6).

TABLE 3. SUMMARY OF EXPERIMENTS AND HORIZONTAL DISPERSION ANALYSIS

Fig 1. The sampler array.

Fig 2. Map of Blashaval showing the approximate positions of experiments 2-9. The tracer release point for each experiment is labelled, and the alignment of the sampler arrays shown at A,B, C.

Fig 3. Map of terrain surrounding Blashaval, after MK85. Spot heights are in metres.

Fig 4. Schematic representation of the velocity profile, flow regions and geometry used in Jackson and Hunt (1975) linear theory.

Fig 5a. Schematic plan of acceptable dispersion experiment. The reduced apparent width of the samper array AB as subtended at the source S results in a slightly exaggerated estimate of dispersion (bias (i)). Near the peak profile, SB is close to but slightly smaller than SQ while SA > SP, giving a slight underestimate of the dispersion (bias (ii)): the two effects are in part compensating.

Fig 5b. As fig 5, but for a rejected experiment. SB, near the peak profile is considerably larger than SQ while SA < SP. The net result is (usually) a substantial over-estimate of dispersion which is further exaggerated by the reduced apparent width of the sampler array due to its angle with the centre-line of the experiment.

Fig 6. Result of Jackson and Hunt (model C) simulation for exp. 2 using digitized Blashaval orography showing hill contours and along- and cross-wind perturbations to the upstream flow at 8m. Negative contours are dashed, and the undisturbed wind is towards the right hand margin.

Contour intervals: u-perturbations 3.64×10^{-2}

v-perturbations 1.59×10^{-2}

where the upstream 8m wind is taken as unity.

Fig 7. Observed concentration profiles (solid lines), corresponding simulations using random walk, formula (15) (- - - -) and reference level terrain profiles from formula (14) (.....).

a) Exps. 2 and 3

b) Exp. 6

c) Exps. 4 and 5

d) Exp. 7

e) Exp. 8

f) Exp. 9

Fig 8. Mean Eulerian vertical displacement of plume for Exp. 6 estimated from a long range random walk simulation. The displacement at $x/z_s = 125$ is about $z/z_s = 0.46$.

Fig 9. Jackson and Hunt model output for Exp 4, to illustrate plume deflection (see text, and caption to fig 6). Note that the v-component of the perturbation is almost congruent (although of opposite phase) to that of the near-orthogonal wind of fig 9.

Contour intervals: u-perturbations 4.41×10^{-2}

v-perturbations 1.62×10^{-2}

for unit undisturbed upstream velocity.

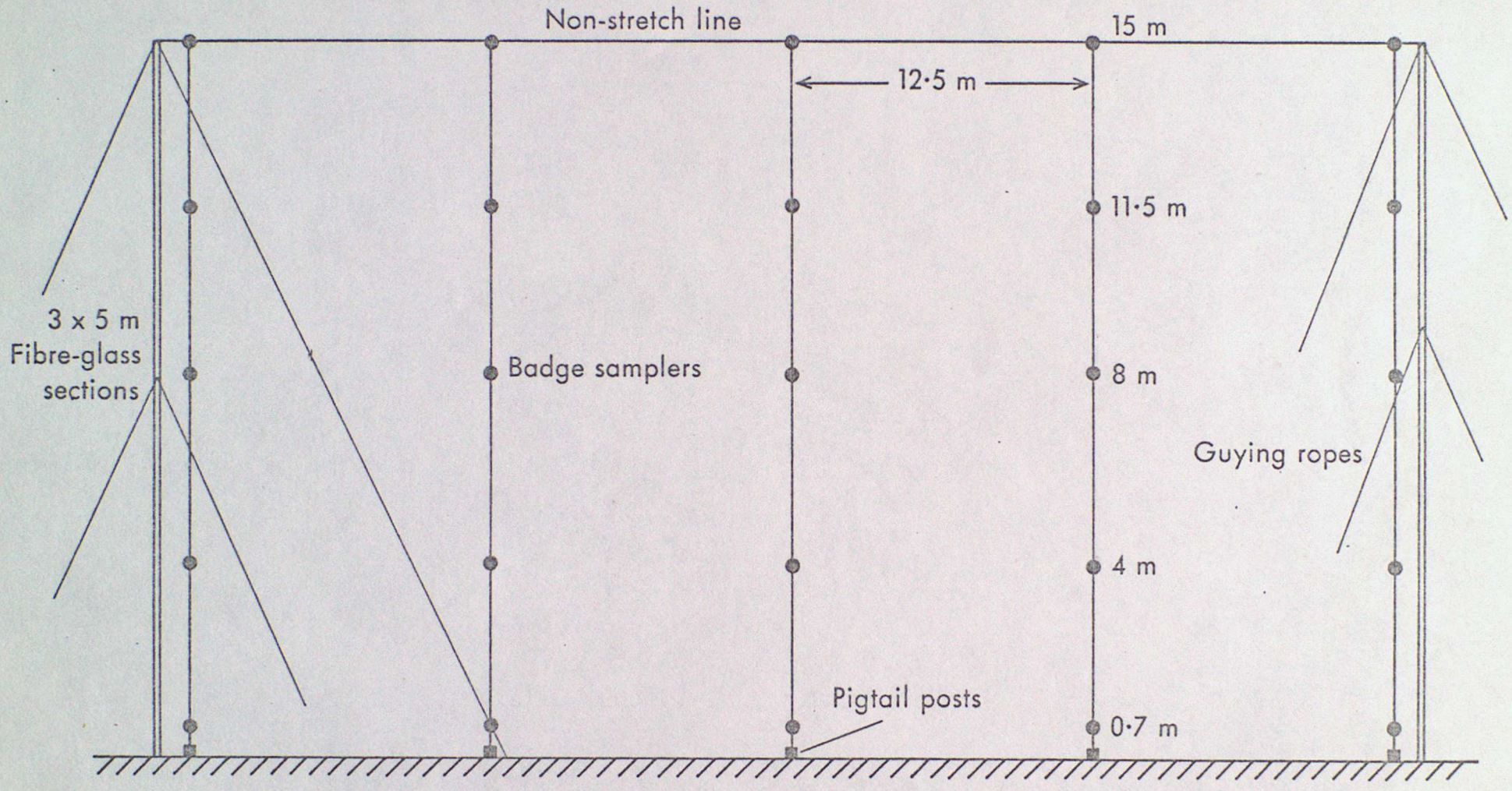

Scale: Horizontal 1:250 Vertical 1:125

FIG 1

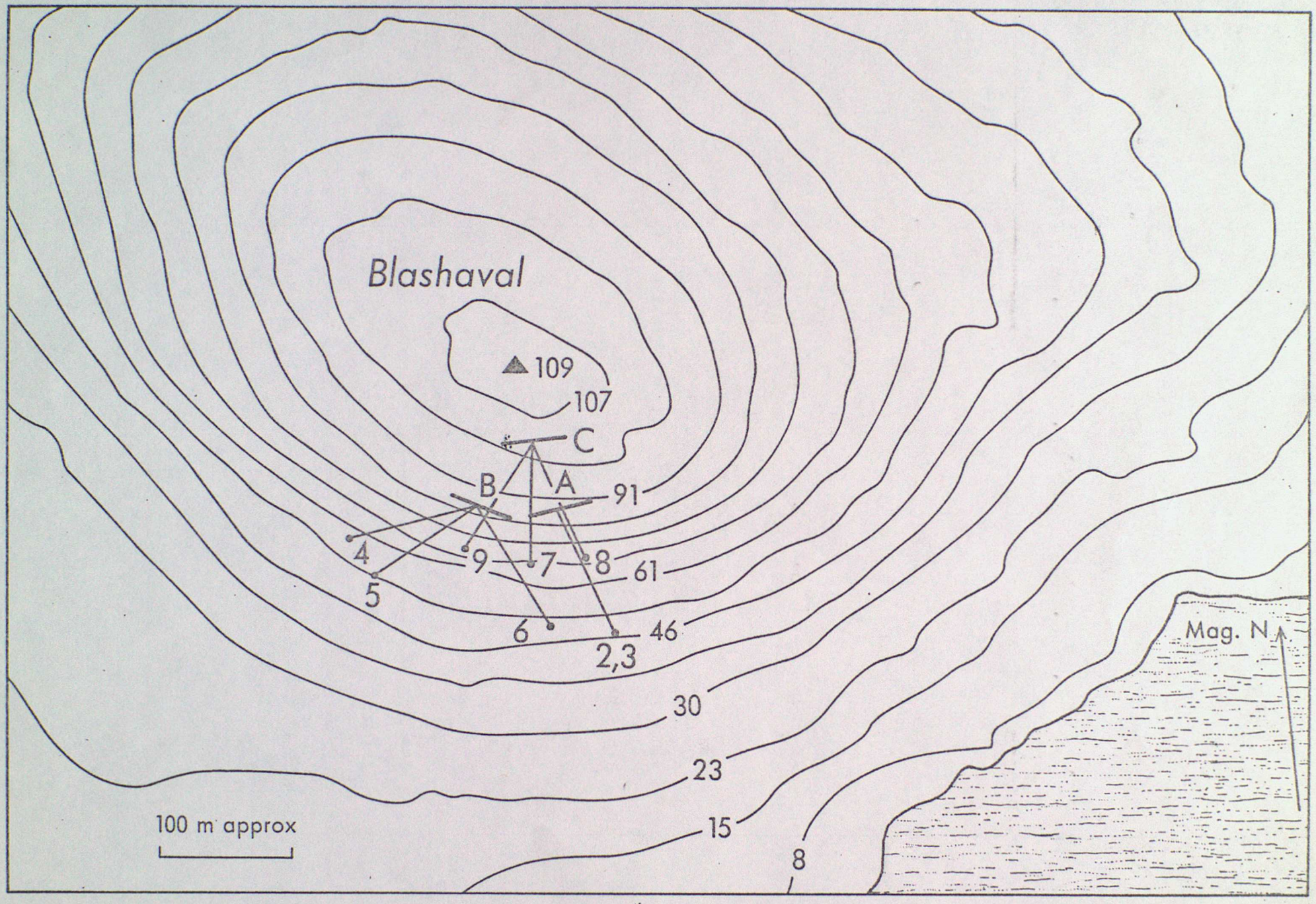
Blashaval
109
107
C
B
A
91
4
9
7
8
61
5
6
46
2,3
30
23
15
8
Mag. N
100 m approx

FIG. 2

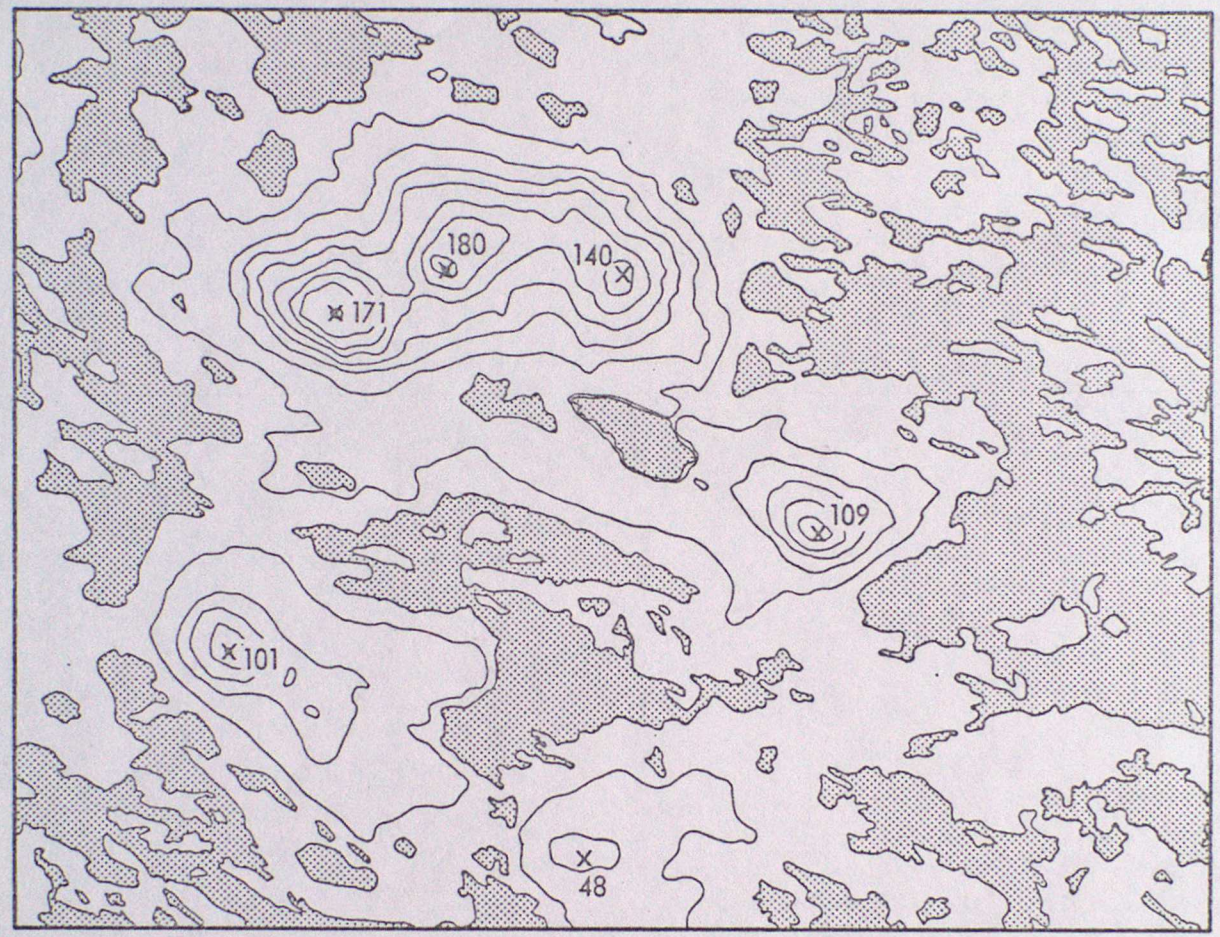

FIG. 3

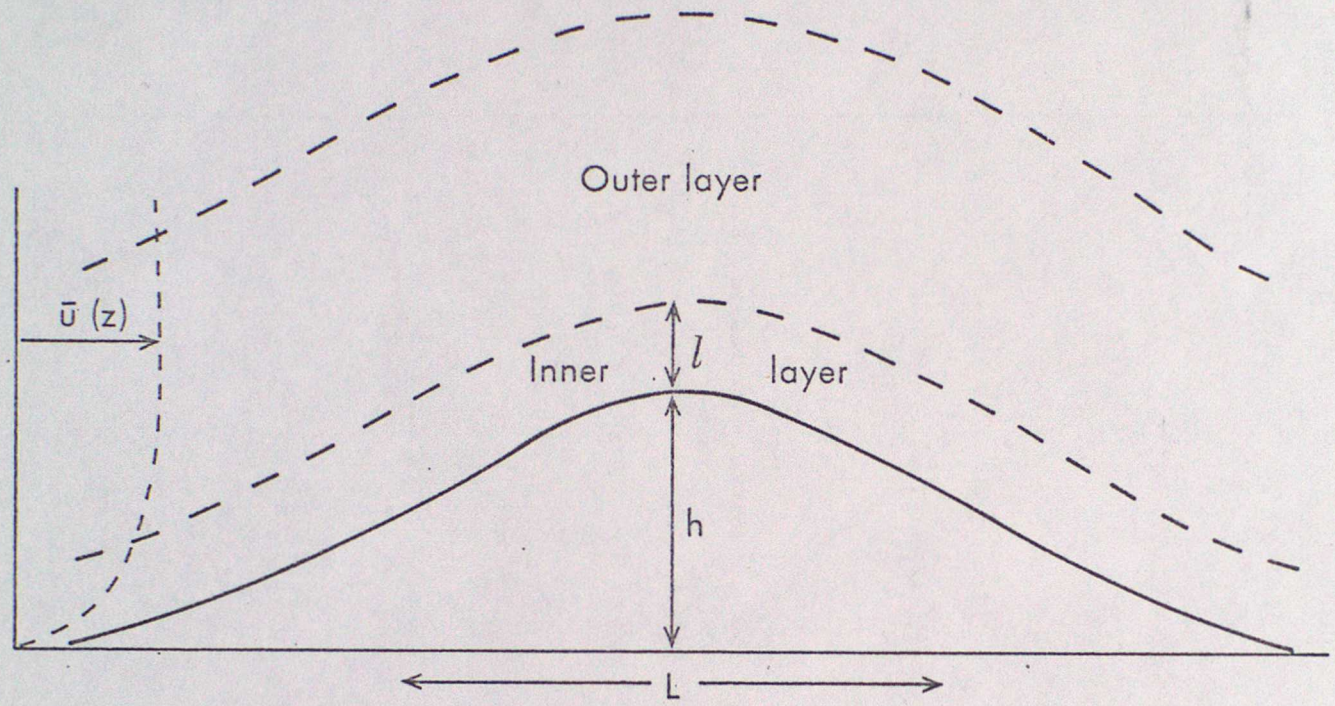

FIG. 4

FIG. 5

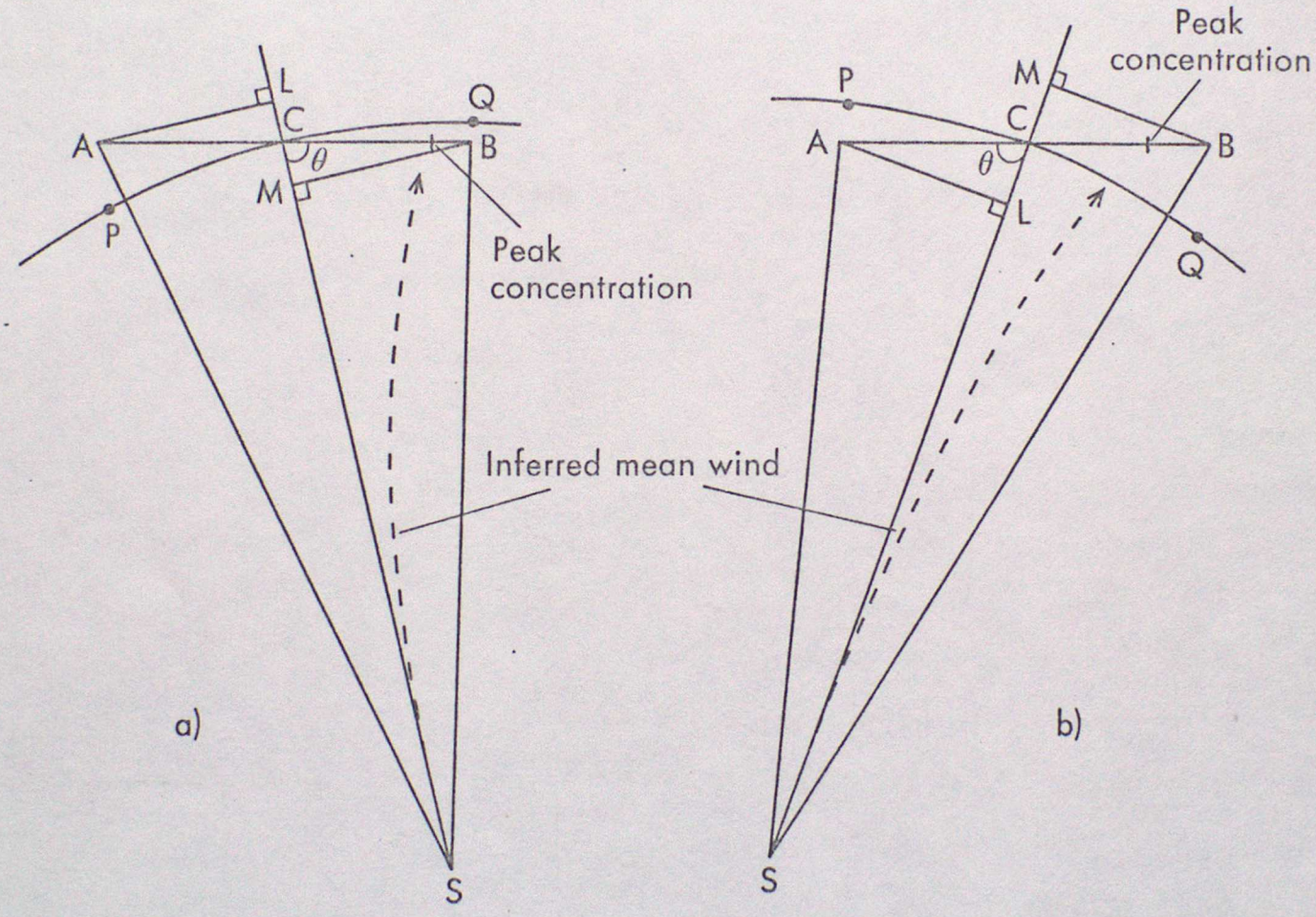

AB is sampler array

S is source

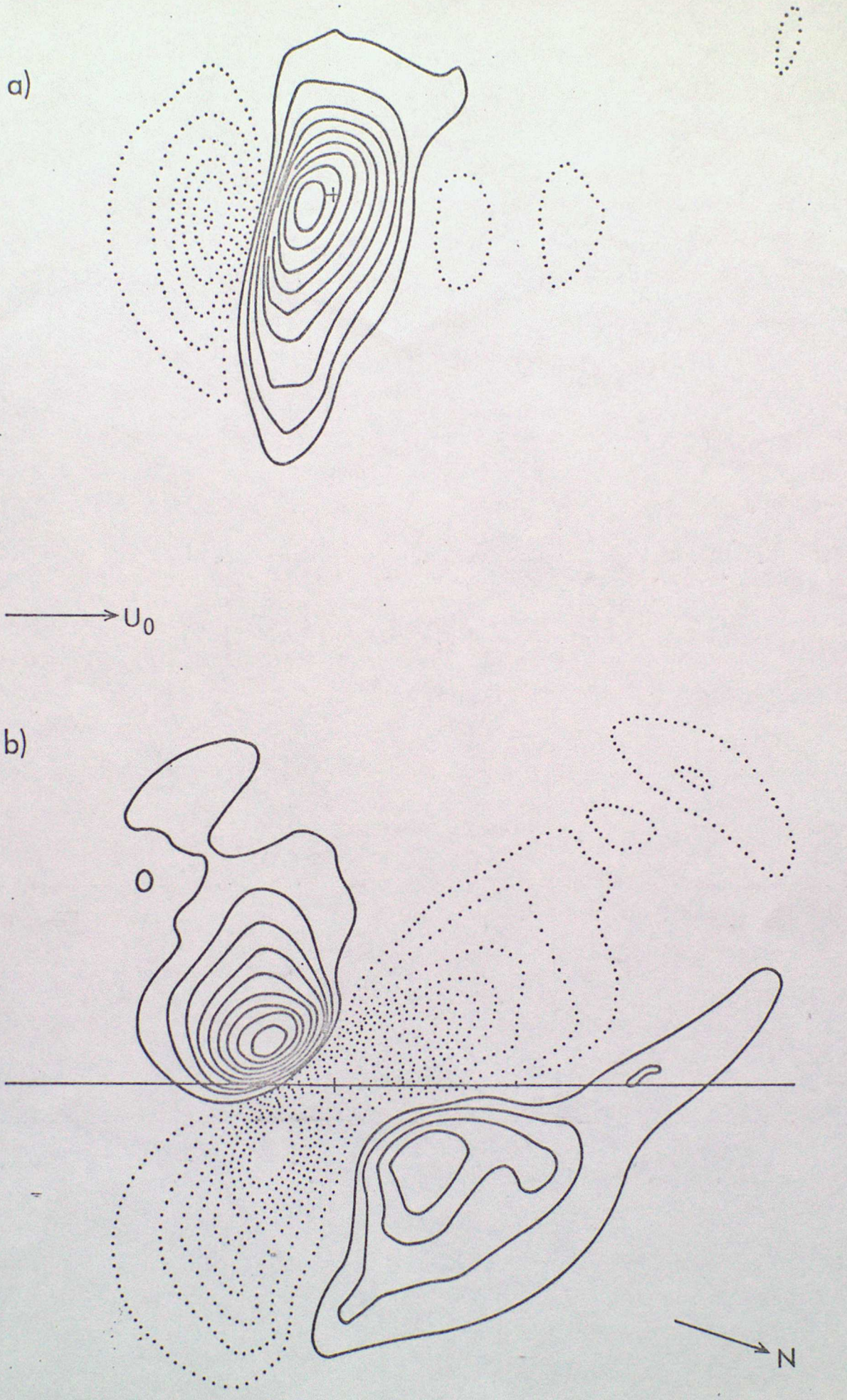

FIG. 6

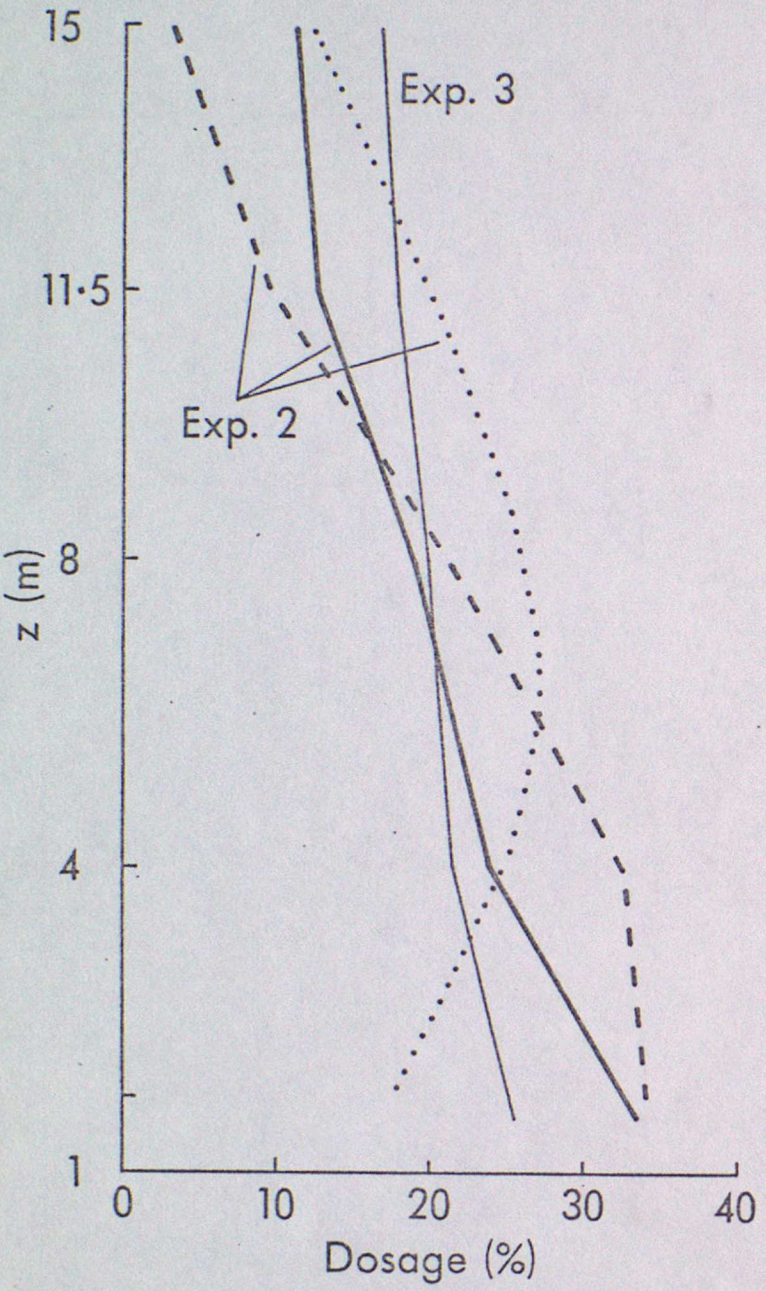
15
11·5
8
4
1
z (m)
Exp. 3
Exp. 2
0
10
20
30
40
Dosage (%)

FIG. 7 a)

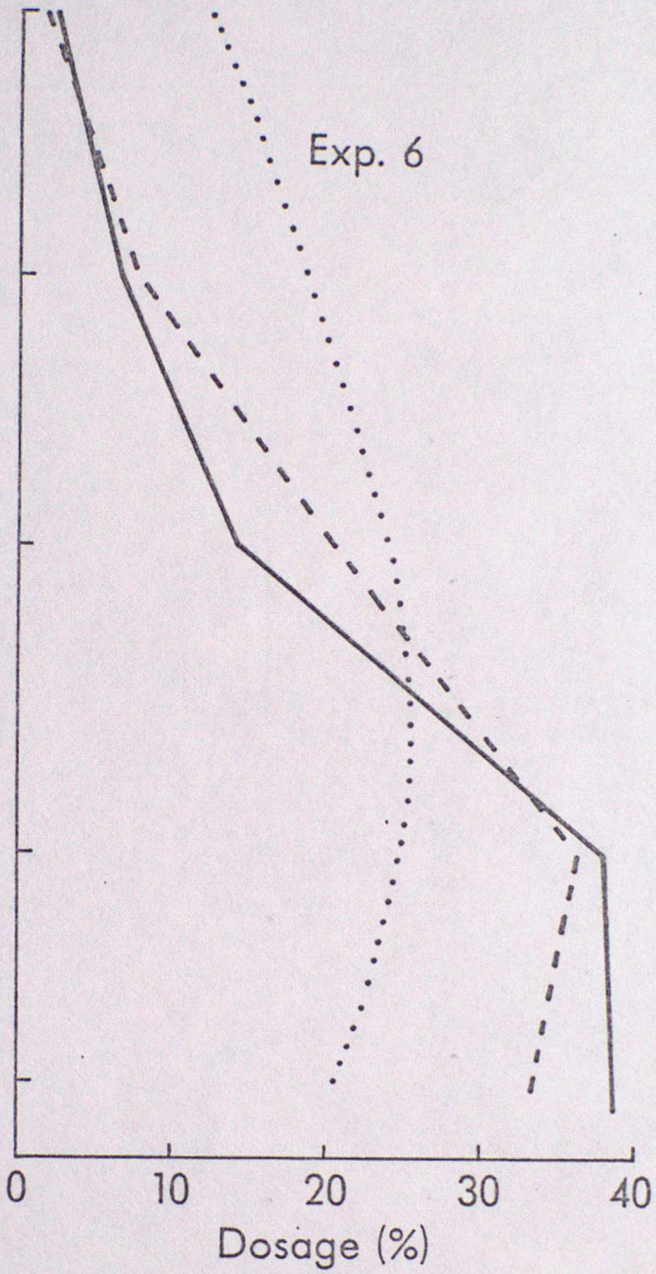
Exp. 6
0
10
20
30
40
Dosage (%)

b)

FIG. 7 c)

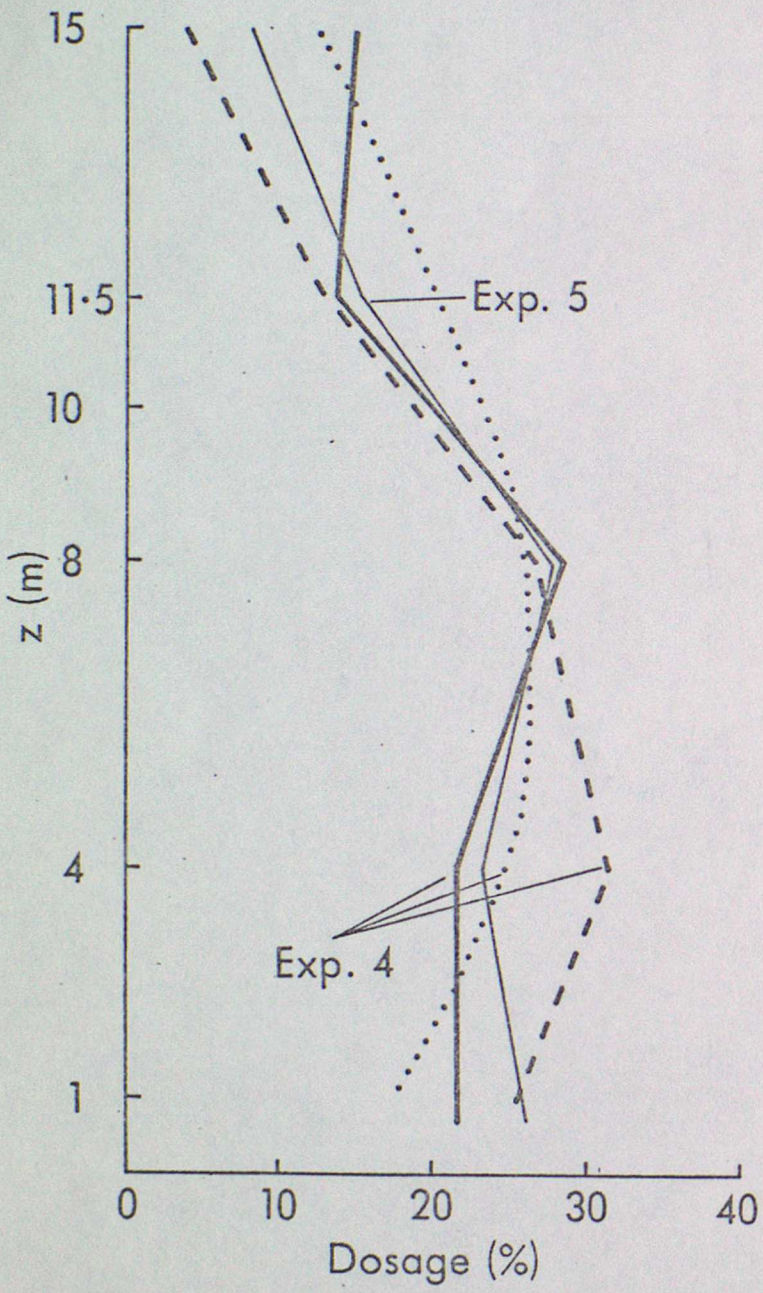
15
11·5
10
8
4
1
z (m)
Exp. 5
Exp. 4
0
10
20
30
40
Dosage (%)

d)

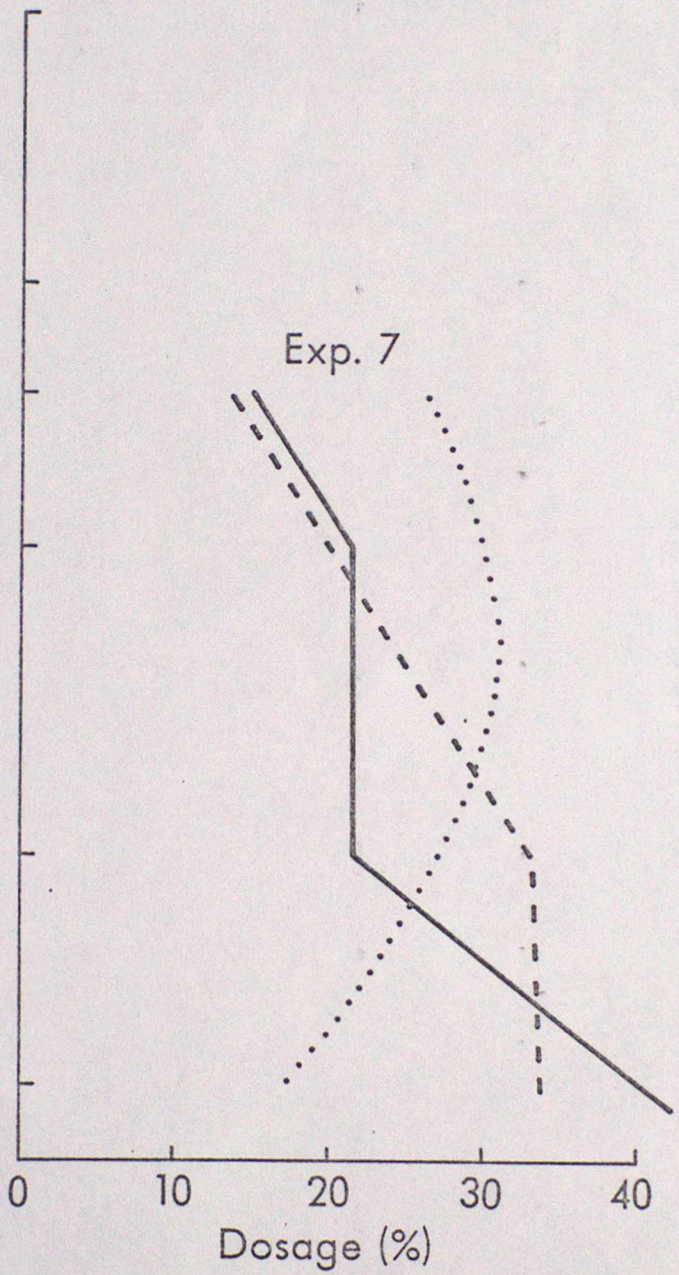
Exp. 7
0
10
20
30
40
Dosage (%)

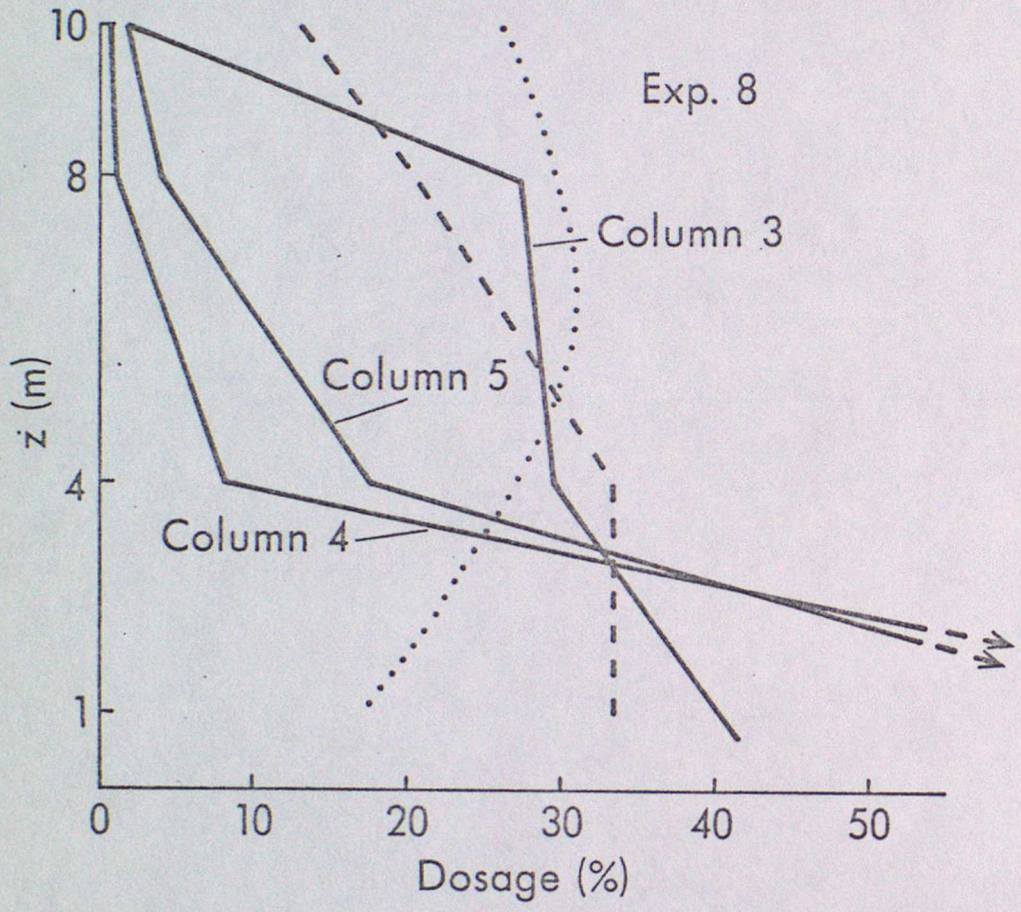
Exp. 8
Column 3
Column 5
Column 4
z (m)
10
8
4
1
0
10
20
30
40
50
Dosage (%)

e)

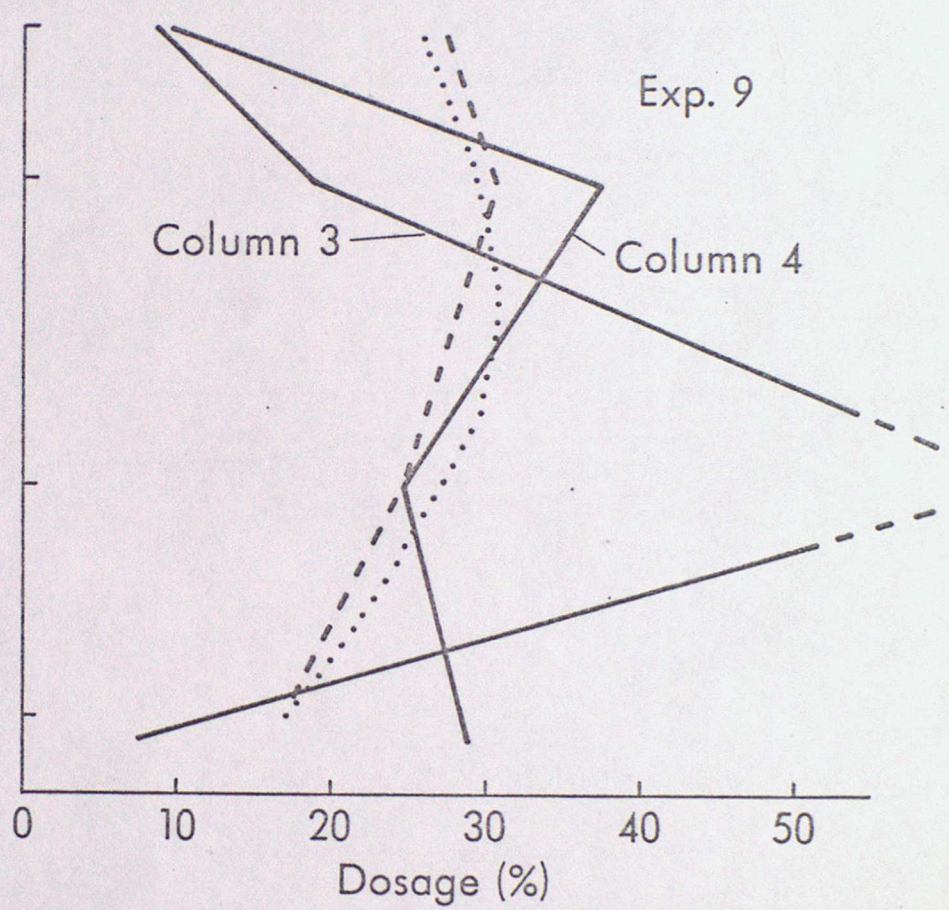
Exp. 9
Column 3
Column 4
0
10
20
30
40
50
Dosage (%)

f)

FIG. 7

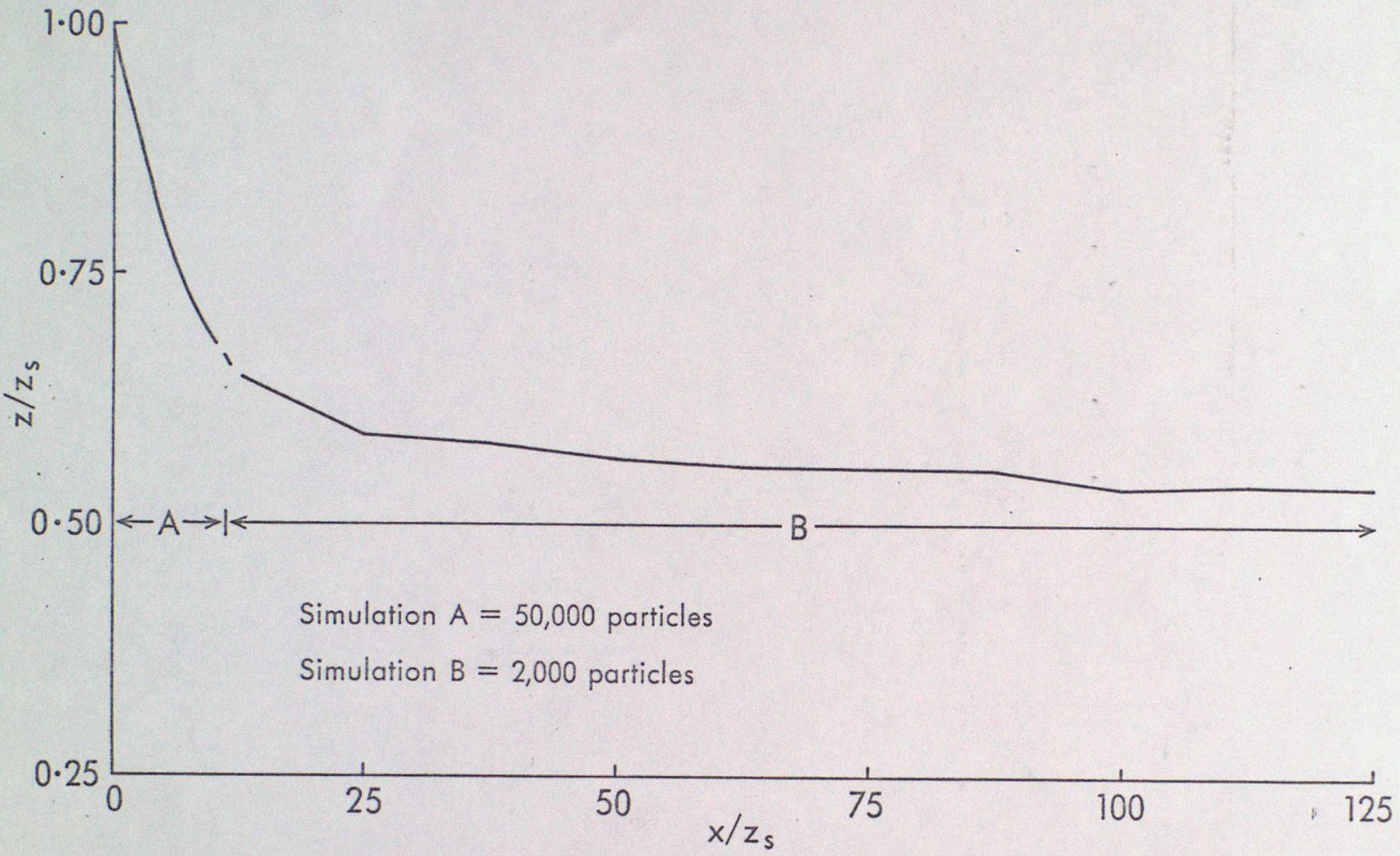
1·00
0·75
0·50
0·25
z/z_s
A
B
Simulation A = 50,000 particles
Simulation B = 2,000 particles
0
25
50
75
100
125
x/z_s

FIG. 8

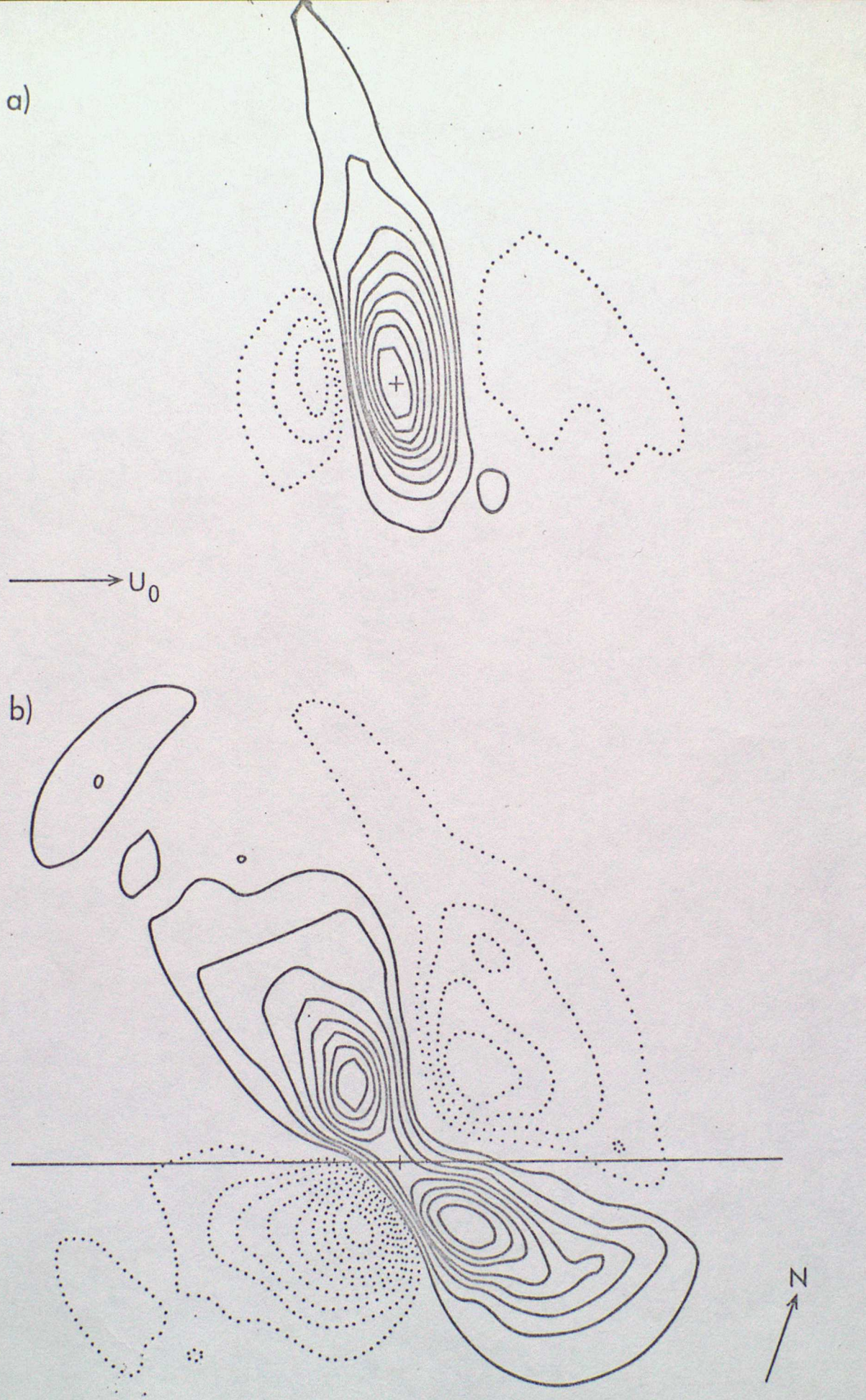

FIG. 9